

Light-Activation of Molecular Motors in Polymersomes

Soumya Kanti Dawn,^{1†} Stefanie Klisch,^{1†} Gerald J. Schneider^{1,2*} Víctor García-López^{1*}

¹ Department of Chemistry, Louisiana State University, Baton Rouge, LA 70803, United States

² Department of Physics & Astronomy, Louisiana State University, Baton Rouge, LA 70803, United States

† Contributed equally

*Corresponding authors: gjschneider@lsu.edu, vglopez@lsu.edu

Table of Contents

List of Abbreviations	3
S1. Materials and General Synthetic Methods.....	4
S2. Synthetic Procedures and Characterization.....	5
S2.1. Compound 4.....	5
S2.2. Compound 5.....	6
S2.3. Compound 6.....	6
S2.4. Compound 12.....	7
S2.5. Compound 13.....	7
S2.6. Compound 14.....	8
S2.7. Compound 15.....	9
S2.8. Compound 7.....	9
S2.9. Compound 8.....	10
S2.10. Synthesis of the Motor 1	11
S2.11. Synthesis of Diblock Copolymer 2.....	12
S3. Polymersome Preparation	15
S4. Dynamic Light Scattering (DLS)	16
S5. Crystal Structure of Motor 1.....	17
S6. Kinetics of the Thermal Helix Inversion (THI) of Motor 1 in Solution.....	25
S6.1. Kinetic Study of the Thermal Helix Inversion (THI) of 1 in Solution by ¹ H NMR.....	25
S6.2. Kinetic Study of the Thermal Helix Inversion (THI) of 1 in Solution by UV-Vis Spectroscopy.....	33

S7. Kinetic Study of the Thermal Helix Inversion (THI) of Motor 1 in Polymersomes	34
S7.1. Procedure for Fitting Absorbance Peaks	35
S8. Effect of Temperature Fluctuations During DLS Measurements	36
S9. NMR Spectra	39

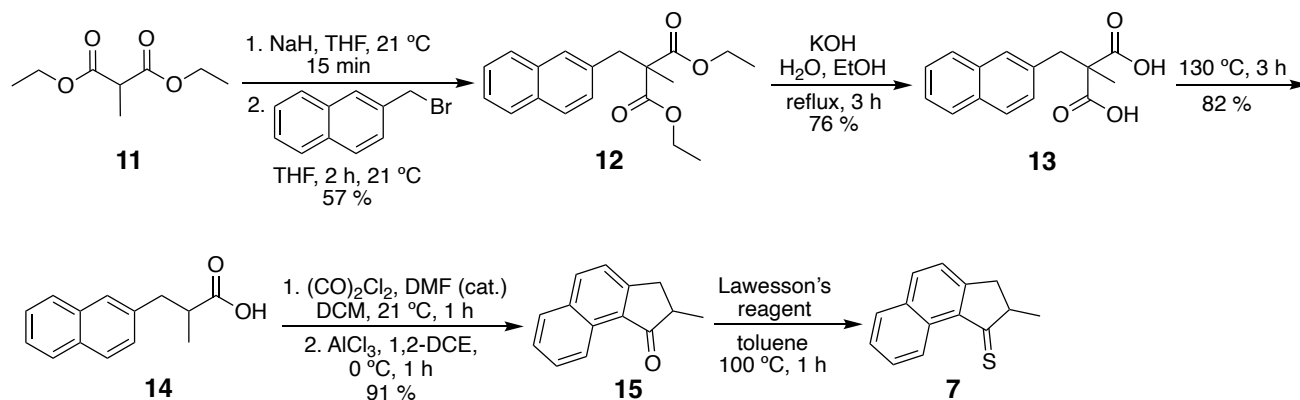
List of Abbreviations

DLS	Dynamic Light Scattering
DMF	N,N-dimethylformamide
DRI	Differential Refractive Index
E.S.D	Estimated Standard Deviation
ESI	Electrospray Ionization
FWHM	Full Width at Half Maximum
GPC	Gel Permeation Chromatography
HFIP	Hexafluoroisopropanol
HPLC	High-performance Liquid Chromatography
HRMS	High-resolution Mass Spectrometry
LED	Light-emitting Diode
LS	Laser Sintering
MALDI	Matrix Assisted Laser Desorption/Ionization
MS	Mass Spectrometry
NMR	Nuclear Magnetic Resonance
PDI	Polydispersity Index
PDMS	Polydimethylsiloxane
PEG	Polyethylene Glycol
PMMA	Poly(methyl methacrylate)
PTFE	Polytetrafluoroethylene
RALS	Right-angle Static Light Scattering
RI	Refractive Index
THF	Tetrahydrofuran
THI	Thermal Helix Inversion

S1. Materials and General Synthetic Methods

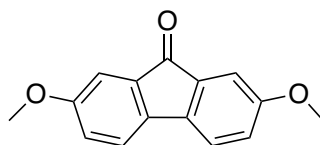
Glassware for the synthesis was oven-dried overnight before use, and the reactions were carried out under a nitrogen atmosphere. All the starting materials were purchased from commercial suppliers as reagent grade and used without further purification unless stated otherwise. PEG **9** and PDMS **10** were purchased from Gelest, Inc. Dry solvents (THF, DMF, CH₃CN, CH₂Cl₂, toluene) were obtained from a solvent purification system from Pure Process Technology under an argon atmosphere. ACS-grade solvents were used for liquid-liquid extractions. Flash column chromatography (FC) was performed using SiO₂ (60 Å, 230-400 mesh, silicycle) at 21 °C and using ACS grade solvents. Thin layer chromatography (TLC) was done using aluminum sheets coated with silica gel 60 F₂₅₄ (Supelco, Sigma Aldrich). Visualization was achieved with UV light (254/365 nm). HPLC-grade solvents were used for the dialysis. ¹H nuclear magnetic resonance (NMR) spectra were recorded on a Bruker AV III 400 at 400 MHz. ¹³C NMR and 2D NMR spectra were recorded on a Bruker AV III 500 spectrometer at 500 MHz. Chemical shifts are reported in ppm using the residual no-deuterated solvent signals as an internal reference (chloroform-d: δ_H = 7.26 ppm, δ_C = 77.16 ppm; methanol-d: δ_H = 3.31 ppm, δ_C = 49.00 ppm; dimethyl sulfoxide-d₆: δ_H = 2.50 ppm, δ_C = 39.52 ppm). For ¹H NMR spectra, coupling constants *J* are given in Hz and the resonance multiplicity is described as s (singlet), d (doublet), t (triplet), m (multiplet), and br (broad). High-resolution Mass Spectra were collected by the LSU MS facility on an Agilent ESI-TOF, a Bruker UltrafleXreme MALDI TOF/TOF, or a Bruker rapifleX MALDI TOF/TOF. 2-[(2E)-3-(4-tert-butylphenyl)-2-methylprop-2-enylidene]malononitrile (DCTB) and α-cyano-4-hydroxycinnamic acid (CHCA) were used as matrix. The most important peaks and clusters are reported in m/z units with [M+H]⁺ (ESI positive mode), [M-H]⁻ (ESI negative mode) and [M]⁺ (MALDI) as the molecular ion.

S2. Synthetic Procedures and Characterization



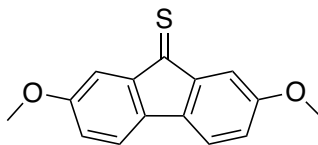
Scheme S1. Synthesis of rotor 7.

S2.1. Compound 4



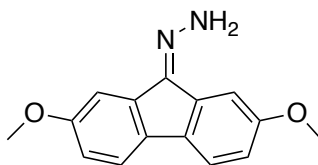
In a 500 mL three-neck round-bottom flask, 2,7-dihydroxyfluorenone **3** (5 g, 23.56 mmol) and K₂CO₃ (13.02 g, 94.25 mmol) were dissolved in dry DMF (30 mL) under nitrogen. The reaction mixture was stirred for 10 min at 55 °C; then, iodomethane (26.75 g, 188.50 mmol) was added, and the mixture was stirred for 16 h at 60 °C. The reaction was then cooled down to room temperature, and HCl (50 mL, 1 N) was added dropwise. The product was extracted with EtOAc (150 mL). The organic layer was concentrated to obtain **4** (5.07 g, 90%) as a red solid. ¹H NMR (400 MHz, chloroform-d): δ = 7.29 (d, *J* = 8.2 Hz, 2H), 7.17 (d, *J* = 2.5 Hz, 2H), 6.94 (dd, *J* = 8.1, 2.5 Hz, 2H), 3.84 (s, 6H); ¹³C NMR (126 MHz, chloroform-d): δ = 193.68, 159.89, 137.41, 135.88, 120.20, 109.53, 55.61; HRMS (ESI) *m/z* calculated for [M+H]⁺ C₁₅H₁₃O₃ 241.0878 found 241.0865.

S2.2. Compound 5



Compound **5** was prepared by modifying a reported procedure.^{S1} Compound **4** (2 g, 8.32 mmol) and Lawesson's reagent (6.73 g, 16.64 mmol, 2 equiv.) were mixed in dry THF (30 mL) under a nitrogen atmosphere in a two-neck 100 mL round-bottom flask. The mixture was refluxed at 66 °C for 1.5 h, then cooled to room temperature. The crude was passed through a 3 cm silica plug, and washed with EtOAc until the eluted solution was colorless. The organic layer was concentrated to afford crude compound **5** as a yellow solid, which was used in the next step without further purification due to its instability.

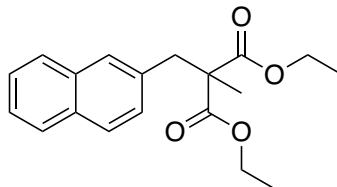
S2.3. Compound 6



Compound **6** was prepared by modifying a reported procedure.^{S2} Compound **5** was dissolved in EtOH (30 mL) in a 100 mL round-bottom flask under a nitrogen atmosphere, then hydrazine monohydrate (2 mL, excess) was added dropwise at 0 °C. The reaction mixture was stirred at 80 °C for 1 h. Upon completion, the mixture was cooled down to room temperature. The solvent was evaporated, and the crude was purified by column chromatography ($R_f = 0.1$, SiO₂; EtOAc/Hex 2:3) to get **6** as a yellow solid (1.76 g, 83%, over two steps). ¹H NMR (400 MHz, chloroform-d): $\delta = 7.55$ (d, $J = 8.3$ Hz, 1H), 7.47 – 7.43 (m, 2H), 7.27 (d, $J = 2.4$ Hz, 1H), 6.95 (dd, $J = 8.3, 2.3$ Hz, 1H), 6.89 (dd, $J = 8.3, 2.4$ Hz, 1H), 6.35 (s, 2H), 3.89 (d, $J = 2.9$ Hz, 6H); ¹³C NMR (126 MHz, chloroform-d): $\delta = 159.52, 158.92, 145.79, 139.36, 134.64, 131.99, 131.58,$

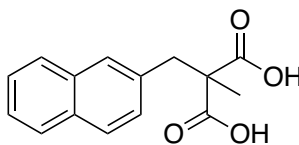
120.32, 119.87, 115.80, 114.06, 113.17, 105.28, 55.93, 55.73; HRMS (ESI) m/z calculated for $[M+H]^+$ $C_{15}H_{15}N_2O_2$ 255.1178 found 255.1132.

S2.4. Compound 12



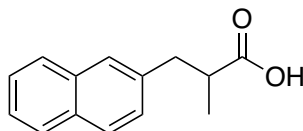
Compound **12** was synthesized by adapting a reported procedure.^{S3} Diethylmethylmalonate **11** (3.0 g, 17.22 mmol) was dissolved in dry THF (60 mL) in a 300 mL three-neck round-bottom flask under a nitrogen atmosphere. Then, 1.6 g (68.88 mmol) of NaH (60% in mineral oil) was added at once, and the mixture was stirred for 15 min at 18 °C. After that, 8.09 g (34.44 mmol) of 2-ethylbromonaphthalene were added at once, and the mixture was stirred for 2 hours at 18 °C. The suspension was filtered, and the orange solution was collected and evaporated. The solid was redissolved in CH_2Cl_2 (50 mL) and washed with H_2O (60 mL). The organic layer was dried over $MgSO_4$ and then concentrated. Purification by column chromatography (R_f = 0.4, SiO_2 gel; EtOAc/Hexane 2:98) gave **12** as a yellow oil (3.08 g, 57%). 1H NMR (400 MHz, chloroform- d , 297 K): δ = 7.82 – 7.71 (m, 3H), 7.60 (s, 1H), 7.49 – 7.39 (m, 2H), 7.24 (d, J = 1.8 Hz, 1H), 4.21 (q, J = 7.1 Hz, 4H), 3.40 (s, 2H), 1.39 (s, 3H), 1.26 (t, J = 7.1 Hz, 6H); ^{13}C NMR (101 MHz, chloroform- d): δ = 172.09, 133.99, 133.44, 132.55, 129.17, 128.54, 127.79, 127.73, 127.69, 126.08, 125.73, 61.48, 55.13, 41.39, 19.99, 14.17; HRMS (ESI) m/z calculated for $[M+H]^+$ $C_9H_{23}O_4$ 315.1578 found 315.1591.

S2.5. Compound 13



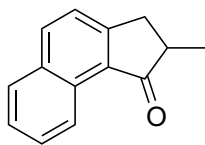
Compound **13** was synthesized by adapting a reported procedure.^{S3} Compound **12** (3.08 g, 9.7 mmol) was dissolved in ethanol (30 mL) under a nitrogen atmosphere in a 250 mL two-neck round-bottom flask, and an aqueous solution of KOH (20 mL, 40 mmol) was added at once. The mixture was refluxed for 3 hours at 95 °C. After cooling the system to 25 °C, the ethanol was evaporated under reduced pressure. The aqueous suspension was stirred, and 0.5 mL of concentrated HCl was added dropwise at 0 °C. A white precipitate was formed, which was filtered, washed with H₂O (50 mL), and dried to afford **13** as a white solid (1.9 g, 76%). ¹H NMR (400 MHz, methanol-d): δ = 7.82 – 7.73 (m, 3H), 7.66 (s, 1H), 7.49 – 7.44 (m, 2H), 7.35 – 7.29 (m, 1H), 3.46 (s, 2H), 1.26 (s, 3H); ¹³C NMR (101 MHz, methanol-d): δ = 175.38, 135.40, 134.61, 133.74, 129.78, 129.37, 128.42, 128.34, 128.31, 126.74, 126.39, 55.73, 42.18, 20.13; HRMS (ESI) m/z calculated for [M-H]⁻ C₁₅H₁₃O₄ 257.0821 found 257.0812.

S2.6. Compound 14



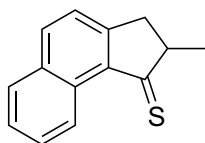
Compound **13** (1.9 g, 7.3 mmol) was heated in a 100 mL round-bottom flask open to air at 130 °C for 4 hours to obtain **14** as a dark brown solid (1.78g, 82%). ¹H NMR (400 MHz, methanol-d): δ = 7.79 (dd, *J* = 10.3, 7.8 Hz, 3H), 7.65 (s, 1H), 7.42 (tt, *J* = 6.8, 5.1 Hz, 2H), 7.35 (dd, *J* = 8.4, 1.8 Hz, 1H), 3.22 – 3.08 (m, 1H), 2.90 – 2.73 (m, 2H), 1.18 (d, *J* = 6.6 Hz, 3H); ¹³C NMR (126 MHz, methanol-d): δ = 179.78, 138.27, 134.87, 133.58, 128.75, 128.39, 128.36, 128.30, 128.22, 126.78, 126.21, 42.45, 40.71, 17.15, 0.81; HRMS (ESI) m/z calculated for [M-H]⁻ C₁₄H₁₃O₂ 213.0921 found 213.0910.

S2.7. Compound 15



Following a reported procedure,^{S4} compound **14** (1.79 g, 8.4 mmol) was dissolved in dry CH₂Cl₂ (30 mL) in a 250 mL one-neck round-bottom flask. Oxalyl chloride (1.42 mL, 16.8 mmol) and then DMF (0.1 mL) were added dropwise under a nitrogen atmosphere. The mixture was stirred for one hour at 18 °C. Afterward, the solvent was evaporated, and the solid was redissolved in dry (CH₂)₂Cl₂ and cooled at 0 °C. AlCl₃ (1.68 g, 12.6 mmol) was added at once, and the mixture was stirred for 1 hour at 100 °C. Upon completion, the mixture was poured into a water/ice mixture, and 0.5 mL of concentrated HCl was added dropwise. The organic layer was extracted with CH₂Cl₂ (60 mL) and washed with H₂O (50 mL). The organic layer was dried over MgSO₄ and then concentrated. The crude product was purified by column chromatography (R_f = 0.3, SiO₂; EtOAc/Hexane 5:95) giving **15** as a pale-yellow oil (1.48g, 91%). ¹H NMR (400 MHz, chloroform-d): δ = 9.16 (d, *J* = 8.3 Hz, 1H), 8.03 (d, *J* = 8.4 Hz, 1H), 7.88 (d, *J* = 8.2 Hz, 1H), 7.71 – 7.62 (m, 1H), 7.55 (t, *J* = 7.6 Hz, 1H), 7.49 (d, *J* = 8.4 Hz, 1H), 3.47 (dd, *J* = 18.1, 8.0 Hz, 1H), 2.82 (d, *J* = 15.0 Hz, 2H), 1.38 (d, *J* = 7.3 Hz, 3H); ¹³C NMR (126 MHz, chloroform-d): δ = 210.19, 156.78, 135.88, 132.85, 130.36, 129.71, 128.99, 128.22, 126.67, 124.09, 42.54, 35.49, 16.78; HRMS (ESI) *m/z* calculated for [M+H]⁺ C₁₄H₁₃O 197.0978 found 197.0967.

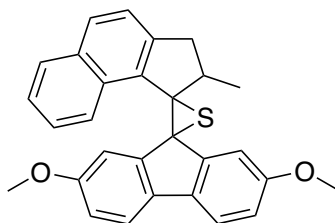
S2.8. Compound 7



Following a reported procedure,^{S4} compound **15** (0.87 g, 4.4 mmol) was dissolved in dry

toluene (25 mL) in a three-neck round bottom flask, and Lawesson's reagent (5.35 g, 13.23 mmol) was added at once. The mixture was refluxed for 1 h at 100 °C under a nitrogen atmosphere. The mixture was cooled to room temperature and passed through a 3 cm silica plug. The silica plug was washed with ethyl acetate until a colorless solution eluted. The purple solution was concentrated under reduced pressure to afford **7** as a dark purple solid (0.91 g). The crude was used in the next step without purification because of its fast decomposition.

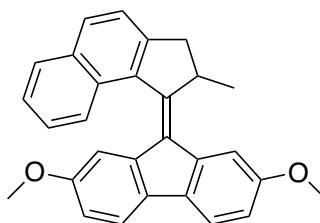
S2.9. Compound 8



By modifying a reported procedure,^{S2} in a 100 mL round-bottom flask, compound **6** (0.9 g, 3.56 mmol) was dissolved in dry THF (20 mL) under a nitrogen atmosphere and cooled to 0 °C. Na₂SO₄ (3 g, 21.12 mmol) and MnO₂ (1.2 g, 14.24 mmol) were added, and the mixture was stirred at 0 °C for 1 h. The suspension was filtered by vacuum filtration and collected in a three-neck round-bottom flask. Thioketone **7** was added to the red filtrate under nitrogen at 0 °C, resulting in the formation of bubbles. The mixture was stirred for 16 h at 18 °C. The solvent was removed under vacuum, and the crude was purified by column chromatography (R_f = 0.2, SiO₂; EtOAc/Hex 3:97) to get **8** as a yellow color solid (0.68 g, 44%). ¹H NMR (400 MHz, chloroform-d): δ = 9.80 (d, *J* = 8.7 Hz, 1H), 7.87 – 7.83 (m, 1H), 7.73 – 7.68 (m, 1H), 7.65 – 7.57 (m, 2H), 7.52 (t, *J* = 8.5 Hz, 2H), 7.43 (ddd, *J* = 8.1, 6.7, 1.2 Hz, 1H), 7.36 (d, *J* = 8.3 Hz, 1H), 7.23 (d, *J* = 8.2 Hz, 1H), 7.04 (d, *J* = 2.4 Hz, 1H), 6.97 – 6.92 (m, 1H), 6.73 (d, *J* = 2.4 Hz, 1H), 6.62 (dd, *J* = 8.3, 2.4 Hz, 1H), 3.93 (s, 3H), 3.21 (p, *J* = 6.7 Hz, 1H), 2.78 (s, 3H), 2.39 (d, *J* = 15.4 Hz, 1H), 1.41 (d, *J* = 7.3 Hz, 1H), 1.28 (d, *J* = 6.8 Hz, 3H); ¹³C NMR (126 MHz, chloroform-d): δ = 158.56, 157.58, 147.36,

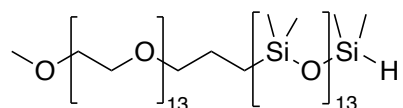
138.26, 136.19, 132.59, 130.94, 129.72, 129.28, 128.73, 127.82, 126.72, 125.23, 124.10, 119.63, 119.33, 118.88, 115.04, 112.32, 110.74, 109.97, 55.69, 54.69, 54.35, 45.17, 41.96, 37.68, 19.48, 19.16; HRMS (ESI) m/z calculated for $[M+H]^+$ $C_{29}H_{25}O_2S$ 437.1578 found 437.1668.

S2.10. Synthesis of the Motor 1



In a 150 mL sealed round-bottom flask, compound **8** (0.37g, 0.84 mmol) and PPh_3 (0.88 g, 3.36 mmol) were dissolved in dry toluene (20 mL) under a nitrogen atmosphere. The mixture was stirred at 130 °C for 16 h. Toluene was evaporated, and the mixture was redissolved in dry CH_3OH . The mixture was stirred for 4 h until motor **1** precipitated. The suspension was filtered, and the solid was washed with CH_3OH and dried to obtain motor **1** as an orange solid (0.15 g, 43%). 1H NMR (400 MHz, chloroform- d): δ = 7.94 (t, J = 8.2 Hz, 2H), 7.82 (d, J = 8.3 Hz, 1H), 7.62 (dd, J = 12.2, 8.3 Hz, 2H), 7.56 – 7.50 (m, 2H), 7.48 (t, J = 7.5 Hz, 1H), 7.40 (td, J = 7.5, 6.6, 1.3 Hz, 1H), 6.95 (dd, J = 8.3, 2.2 Hz, 1H), 6.77 (dd, J = 8.3, 2.3 Hz, 1H), 6.27 (d, J = 2.3 Hz, 1H), 4.36 (p, J = 6.6 Hz, 1H), 3.96 (d, J = 1.0 Hz, 3H), 3.61 (dd, J = 15.2, 5.7 Hz, 1H), 2.97 (s, 2H), 2.80 (d, J = 15.1 Hz, 1H), 1.42 (s, 1H). ^{13}C NMR (126 MHz, chloroform- d): δ = 158.58, 157.60, 151.03, 147.35, 141.08, 138.26, 136.20, 133.71, 132.92, 132.60, 130.94, 130.64, 129.73, 128.72, 127.82, 126.72, 125.23, 124.09, 119.32, 118.87, 115.05, 112.31, 110.75, 109.99, 77.28, 77.03, 76.77, 55.69, 54.35, 45.18, 41.96, 19.16. HRMS (ESI) m/z calculated for $[M+H]^+$ $C_{29}H_{25}O_2$ 405.1878 found 405.1871.

S2.11. Synthesis of Diblock Copolymer



Copolymer **2** was prepared by modifying a reported procedure,^{S5} PEG **9** (0.52 g, 1.04 mmol, 1.1 equiv.) and PDMS **10** (0.93 g, 0.93 mmol, 1 equiv.), Karstedt's catalyst (0.1 equiv.) and toluene (10 mL) were added to a round-bottom flask under a nitrogen atmosphere. The mixture was stirred for 16 h at 70 °C. The mixture was cooled to 25 °C, and the toluene was evaporated. The dried oily mixture was dissolved in HPLC grade CH₃OH with a concentration of 60 mg/mL, and poured into a 1KD dialysis bag of 7 cm. The bag was dipped in a 1000 mL beaker containing CH₃OH (950 mL, HPLC grade). The system was agitated gently by using a mechanical stirrer for 20 h. Afterward, the fraction left in the dialysis bag was collected and CH₃OH was evaporated. The gel with the suspension of catalyst was dissolved in hexane and filtered through a 1 μm filter to remove the catalyst. Hexane was evaporated to get the diblock copolymer **2** as a transparent oil (650 mg). The completion of the reaction was confirmed by the disappearance of the vinylic H peaks of PEG (**Figure S1**), which was observed in the synthesis of similar copolymers.^{S5} Moreover, the formation of the diblock copolymer was further verified by MALDI- MS (**Figure S2**). Furthermore, polydispersity index (PDI) was found to be 1.18 by performing gel permeation chromatography (GPC) (**Figure S3**).

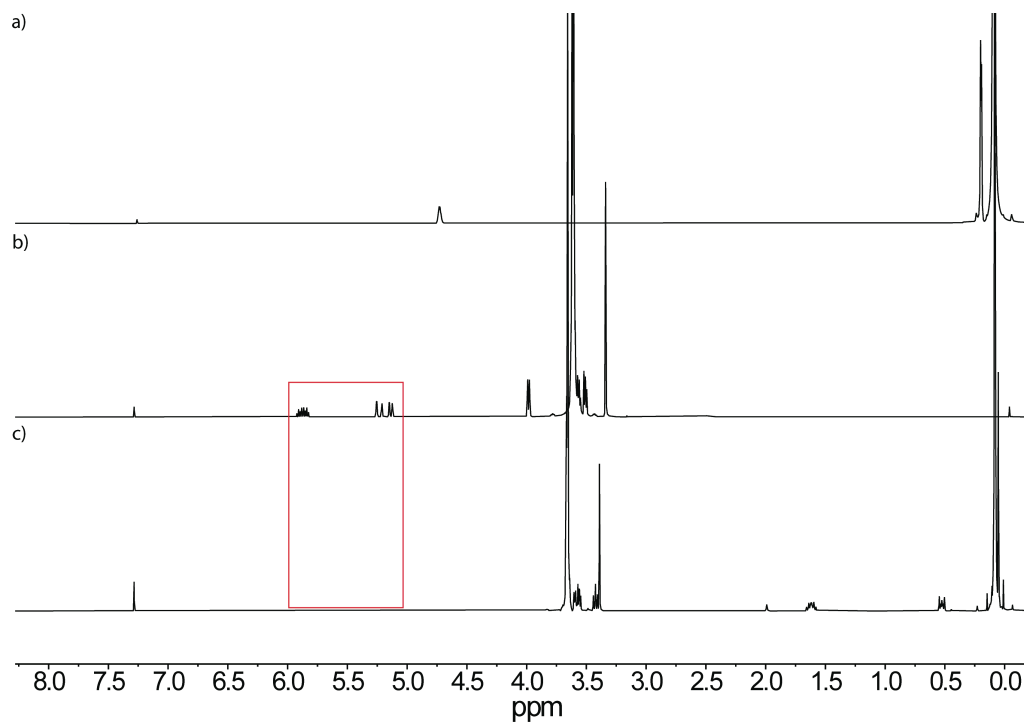


Figure S1. ^1H NMR spectra of (a) PDMS **10**, (b) PEG **9**, and (c) diblock copolymer **2** in chloroform-d (400 MHz, $T = 297$ K). The highlighted peaks correspond to the vinylic -H of the PEG **14**, which disappears after the formation of the diblock copolymer **2**.

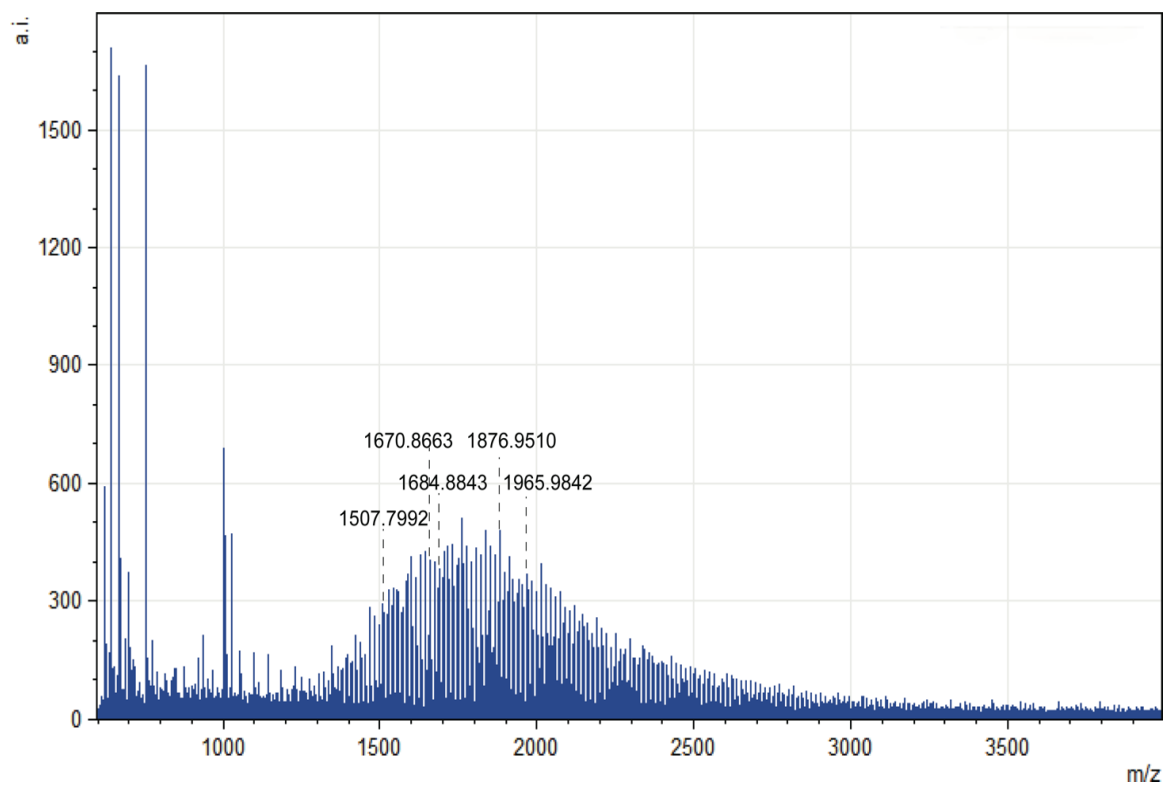


Figure S2. MALDI-MS of diblock copolymer **2**.

Molecular Weight Distribution Study of 2

Size-exclusion chromatography (SEC) analysis was performed using a Tosoh Bioscience EcoSECelite system (Tosoh Bioscience degasser, isocratic pump, autosampler, and column heater) equipped with two TSKgel Alpha-M 13 μm , 7.8 mm ID \times 30 cm columns, a Tosoh Bioscience dual flow RI detector with a 630–670 nm LED light source, and a Tosoh Bioscience LenS 3 multiangle light scattering (MALS) detector (30 mW diode laser at $\lambda = 505$ nm). HFIP with 3 mg/mL $\text{CF}_3\text{CO}_2\text{K}$ was used as the eluent at a flow rate of 0.450 mL/min. The pump housing, column oven, and RI detector temperatures were set at 40 °C. All data analysis was performed using SEC view software. Polymer molecular weight and molecular weight distribution were obtained by analyzing the RALS-DRI data based on the LS and RI instrument constants that were calibrated with a PMMA standard (M_w (LS) = 32350 g/mol, PDI = 1.03) in HFIP/ $\text{CF}_3\text{CO}_2\text{K}$ (3 mg/mL) with known concentration. The refractive index increment (dn/dc) of the polymer was determined to be 0.183 mL/g in HFIP/ $\text{CF}_3\text{CO}_2\text{K}$ (3 mg/mL) at 40°C. The sample was prepared in 1 mg/mL concentration in HFIP, and it was left overnight to ensure dissolution. The sample solution was filtered through a 0.45 micron PTFE filter prior to sample injection.

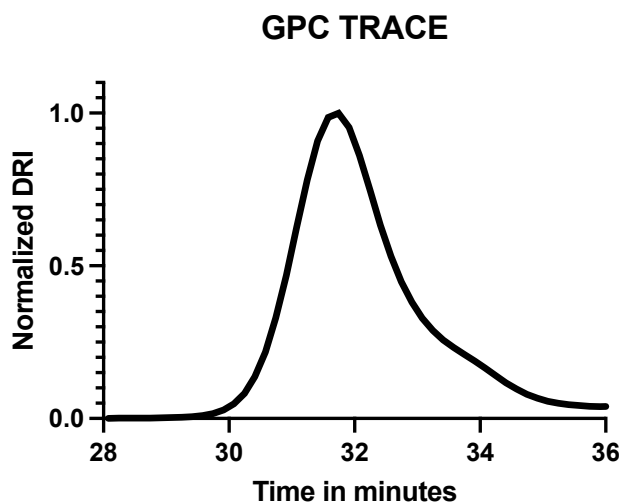


Figure S3. GPC analysis of diblock copolymer 2. PDI = 1.18.

S3. Polymersome Preparation

Motor **1** was incorporated into the polymersome by following a procedure previously published by De Mel et al.^{S6} Stock solutions of 0.01 mol L⁻¹ PDMS₁₃-*b*-PEG₁₃ diblock copolymer and 0.001 mol L⁻¹ motor **1** were prepared using EtOH as a solvent. 5 × 10⁻³ mol PDMS₁₃-*b*-PEG₁₃ diblock copolymer was assigned the value of 100. Mole proportions of 100:0, 100:0.5, 100:1 and 100:2 were then prepared by mixing the appropriate amount of the polymer stock solution with the motor stock solution. The solvent was evaporated under an N₂ stream, and the sample was dried overnight in a vacuum oven at an ambient temperature. The samples were then rehydrated with 1 mL ultrapure water 18.2 MΩ and subjected to four freeze-thaw cycles (-20 °C for 10 min then 50 °C for 10 min per cycle). Next, the samples were sonicated using a Sonic VibraCell VC-750 Sonicator at 20 % amplitude with a pulse program of 1.0 s off and 0.5 s on for a total of 30 s at a sanitation frequency of 20 kHz. Following sonication, the samples were extruded three times through a 100 nm membrane and filtered through a 0.45 μm syringe filter before use. **Table S1** shows the amounts of motor **1** and diblock copolymer **2** stock used to prepare the polymersomes with intercalated motor. 0.001 mol L⁻¹ of **1** and 0.01 mol L⁻¹ of **2** were used to prepare the polymersomes incorporated with motor **1**. For kinetics studies in solution, 1.0 × 10⁻⁴ mol L⁻¹ of **1** were dissolved directly in the solvent.

Table S1. Volumes of stock concentrations used to prepare a 1 mL sample of polymersomes incorporated with motor **1**. The stock solutions contain 0.01 mol L⁻¹ of diblock copolymer **2** and 0.001 mol L⁻¹ of **1**.

Diblock copolymer: motor molar ratio	V 2 Stock (mL)	V 1 Stock (mL)	[2] (mol L ⁻¹)	[2] (mol L ⁻¹)
100:0	0.537	0.000	5.4 × 10 ⁻³	0
100:0.5	0.537	0.027	5.4 × 10 ⁻³	2.7 × 10 ⁻⁵
100:1	0.537	0.054	5.4 × 10 ⁻³	5.4 × 10 ⁻⁵
100:2	0.537	0.107	5.4 × 10 ⁻³	1.0 × 10 ⁻⁴

S4. Dynamic Light Scattering

All light scattering experiments were performed using Malvern Zetasizer Nano ZS running a 633 nm, 30 mW He-Ne laser and a scattering angle $\theta = 173^\circ$. All measurements were carried out at 22 °C, unless otherwise stated. An equilibration time of 15 min was used for experiments at non-ambient temperatures. Three runs were recorded at each temperature, and the hydrodynamic diameter (D_H) was calculated from the diffusion coefficient via the Stokes-Einstein equation.

$$D_H = \frac{k_B T}{3\pi\eta_0 D} \quad (\text{S1})$$

Where, k_B is the Boltzmann Constant, T is the temperature, η_0 is the solvent viscosity (H₂O) and D is the Diffusion Coefficient. The three recorded values were then averaged to obtain the D_H . For time-independent measurements, twelve scans of 10 s length were recorded. For time- dependent measurements, six scans of 10 s length were recorded.

Light irradiation increased the temperature of the sample from 22 to 24 °C, thus, the DLS measurements for those samples were done at 24 °C to avoid temperature fluctuations that could give erroneous D_H values. Further explanation is discussed in **Section S8**.

S5. Crystal Structure of Motor 1

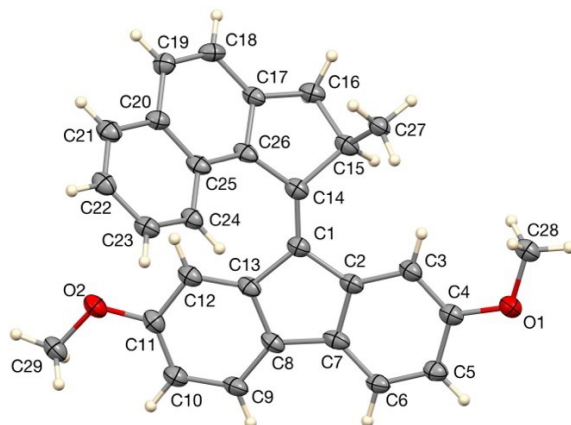


Figure S4. Single crystal structure of motor 1.

Computing details

Data collection: Bruker *APEX3*; cell refinement: Bruker *S SAINT*; data reduction: Bruker *S SAINT*; program(s) used to solve structure: *SHELXT* 2014/5 (Sheldrick, 2014); program(s) used to refine structure: *SHELXL*2018/1 (Sheldrick, 2018).

CCDC 2280653 contains the supplementary crystallographic data for this paper, including structure factors and refinement instructions. These data can be obtained free of charge from The Cambridge Crystallographic Data Centre, 12 Union Road, Cambridge CB2 1EZ, UK.

Crystal data

C₂₉H₂₄O₂

$M_r = 404.48$

Monoclinic, $P2_1/n$

$a = 8.8235 (11) \text{ \AA}$

$b = 11.4469 (12) \text{ \AA}$

$c = 20.836 (3) \text{ \AA}$

$\beta = 100.564 (10)^\circ$

$V = 2068.8 (4) \text{ \AA}^3$

$Z = 4$

$F(000) = 856$

$D_x = 1.299 \text{ Mg m}^{-3}$

Cu $K\alpha$ radiation, $\lambda = 1.54184 \text{ \AA}$

Cell parameters from 1325 reflections

$2\theta = 4.3\text{--}62.6^\circ$

$\mu = 0.63 \text{ mm}^{-1}$

$T = 100 \text{ K}$

Lath, orange

$0.18 \times 0.08 \times 0.01 \text{ mm}$

Data collection

Bruker Kappa APEX-II DUO
diffractometer

19834 independent reflections

Radiation source: I μ S microfocus
QUAZAR multilayer optics monochromator

6666 reflections with $I > 2\sigma(I)$

ϕ and ω

$\theta_{\max} = 64.2^\circ$, $\theta_{\min} = 4.3^\circ$

Absorption correction: multi-scan

$h = -9\text{--}10$

SADABS^{S7}

$k = -13\text{--}13$

$T_{\min} = 0.773$, $T_{\max} = 0.994$

$l = -21\text{--}24$

19834 measured reflections

Refinement

Refinement on F^2

0 restraints

Least-squares matrix: full

Hydrogen site location: inferred from
neighbouring sites

$R[F^2 > 2\sigma(F^2)] = 0.138$

H-atom parameters constrained

$wR(F^2) = 0.526$

$w = 1/[\sigma^2(F_o^2) + (0.1P)^2]$

$S = 0.93$

where $P = (F_o^2 + 2F_c^2)/3$

19834 reflections

$(\Delta/\sigma)_{\max} < 0.001$

284 parameters

$\Delta\rho_{\max} = 0.36 \text{ e \AA}^{-3}$

$\Delta\rho_{\min} = -0.42 \text{ e \AA}^{-3}$

Special details

Geometry. All e.s.d.'s (except the e.s.d. in the dihedral angle between two l.s. planes) are estimated using the full covariance matrix. The cell e.s.d.'s are taken into account individually in the estimation of e.s.d.'s in distances, angles and torsion angles; correlations between e.s.d.'s in cell parameters are only used when they are defined by crystal symmetry. An approximate (isotropic) treatment of cell e.s.d.'s is used for estimating e.s.d.'s involving l.s. planes.

Refined as a 2-component twin.

Fractional atomic coordinates and isotropic or equivalent isotropic displacement parameters (\AA^2)

	<i>x</i>	<i>y</i>	<i>z</i>	$U_{\text{iso}}^*/U_{\text{eq}}$
O1	0.3061 (10)	0.4527 (7)	0.8685 (4)	0.049 (2)
O2	0.7826 (11)	0.8231 (7)	0.5440 (4)	0.051 (2)
C1	0.5823 (14)	0.5291 (9)	0.6811 (6)	0.040 (3)
C2	0.4958 (14)	0.5526 (9)	0.7345 (6)	0.042 (3)
C3	0.4384 (15)	0.4746 (10)	0.7765 (7)	0.046 (3)
H3	0.448885	0.394266	0.772305	0.055*
C4	0.3659 (14)	0.5215 (10)	0.8241 (6)	0.045 (3)
C5	0.3542 (15)	0.6412 (10)	0.8328 (7)	0.048 (3)
H5	0.307873	0.669843	0.866185	0.057*
C6	0.4110 (15)	0.7174 (10)	0.7920 (7)	0.045 (3)
H6	0.402494	0.797714	0.797289	0.054*
C7	0.4816 (14)	0.6725 (10)	0.7427 (7)	0.046 (3)
C8	0.5571 (14)	0.7333 (9)	0.6953 (6)	0.043 (3)
C9	0.5720 (16)	0.8503 (10)	0.6812 (7)	0.050 (4)
H9	0.530501	0.906731	0.705014	0.060*
C10	0.6486 (16)	0.8840 (10)	0.6316 (7)	0.049 (3)
H10	0.661547	0.962748	0.623132	0.058*
C11	0.7051 (15)	0.8000 (10)	0.5950 (7)	0.047 (3)
C12	0.6912 (14)	0.6810 (10)	0.6070 (7)	0.046 (3)
H12	0.727587	0.625555	0.580952	0.055*
C13	0.6218 (14)	0.6470 (9)	0.6587 (6)	0.041 (3)

Continued...

Continued...

C14	0.6094 (14)	0.4232 (10)	0.6563 (6)	0.041 (3)
C15	0.5103 (15)	0.3132 (10)	0.6592 (7)	0.046 (3)
H15	0.407815	0.334592	0.667152	0.055*
C16	0.4999 (15)	0.2664 (10)	0.5889 (7)	0.048 (3)
H16A	0.487396	0.182217	0.587482	0.058*
H16B	0.414577	0.301973	0.559388	0.058*
C17	0.6535 (14)	0.3020 (9)	0.5718 (6)	0.042 (3)
C18	0.7323 (16)	0.2548 (10)	0.5249 (6)	0.046 (3)
H18	0.686177	0.197258	0.496349	0.056*
C19	0.8775 (14)	0.2940 (10)	0.5216 (6)	0.044 (3)
H19	0.929206	0.264135	0.490095	0.053*
C20	0.9491 (14)	0.3805 (9)	0.5662 (6)	0.043 (3)
C21	1.1020 (16)	0.4173 (10)	0.5639 (7)	0.052 (4)
H21	1.152777	0.387605	0.532071	0.062*
C22	1.1738 (15)	0.4960 (10)	0.6082 (7)	0.049 (3)
H22	1.272980	0.520988	0.605866	0.058*
C23	1.0997 (15)	0.5400 (10)	0.6574 (7)	0.047 (3)
H23	1.152476	0.589393	0.689286	0.057*
C24	0.9512 (14)	0.5103 (10)	0.6584 (6)	0.041 (3)
H24	0.901690	0.542780	0.689900	0.050*
C25	0.8694 (14)	0.4303 (9)	0.6120 (6)	0.044 (3)
C26	0.7169 (14)	0.3930 (9)	0.6124 (6)	0.043 (3)
C27	0.5840 (15)	0.2221 (9)	0.7085 (6)	0.045 (3)
H27A	0.677020	0.193600	0.696284	0.067*
H27B	0.513611	0.158400	0.709274	0.067*
H27C	0.607882	0.256928	0.751100	0.067*
C28	0.3222 (16)	0.3300 (10)	0.8622 (7)	0.049 (3)
H28A	0.286371	0.307610	0.817581	0.073*
H28B	0.262372	0.290674	0.889708	0.073*
H28C	0.428742	0.308843	0.874978	0.073*
C29	0.7945 (17)	0.9426 (11)	0.5251 (7)	0.056 (4)
H29A	0.693460	0.972675	0.508344	0.084*
H29B	0.856830	0.947407	0.491997	0.084*
H29C	0.841138	0.987684	0.562394	0.084*

Atomic displacement parameters (\AA^2)

	U^{11}	U^{22}	U^{33}	U^{12}	U^{13}	U^{23}
O1	0.053 (6)	0.038 (5)	0.056 (6)	-0.007 (4)	0.013 (4)	-0.002 (4)
O2	0.058 (6)	0.035 (4)	0.060 (6)	-0.002 (4)	0.009 (5)	0.008 (4)
C1	0.039 (7)	0.033 (6)	0.046 (8)	0.000 (5)	0.002 (6)	-0.001 (5)
C2	0.039 (7)	0.032 (6)	0.053 (8)	-0.002 (5)	0.002 (6)	-0.003 (5)
C3	0.044 (8)	0.033 (6)	0.060 (9)	-0.002 (5)	0.008 (6)	-0.001 (5)
C4	0.043 (8)	0.036 (7)	0.053 (9)	-0.001 (5)	0.003 (6)	-0.002 (6)
C5	0.049 (8)	0.036 (6)	0.058 (9)	0.004 (5)	0.009 (6)	-0.003 (6)
C6	0.043 (8)	0.031 (6)	0.059 (9)	0.000 (5)	0.008 (6)	-0.008 (5)
C7	0.036 (7)	0.032 (6)	0.065 (9)	-0.001 (5)	-0.003 (6)	-0.006 (6)
C8	0.040 (7)	0.029 (6)	0.055 (8)	-0.001 (5)	-0.001 (6)	0.005 (5)
C9	0.052 (8)	0.029 (6)	0.068 (9)	-0.004 (5)	0.008 (7)	-0.008 (6)
C10	0.053 (9)	0.035 (7)	0.056 (9)	0.000 (5)	0.006 (7)	0.001 (6)
C11	0.046 (8)	0.039 (7)	0.054 (9)	-0.002 (5)	0.005 (7)	0.008 (6)
C12	0.041 (8)	0.034 (7)	0.059 (9)	0.000 (5)	0.003 (7)	0.000 (5)
C13	0.035 (7)	0.030 (6)	0.056 (8)	0.004 (5)	0.003 (6)	0.004 (5)
C14	0.036 (7)	0.035 (6)	0.049 (8)	0.001 (5)	-0.001 (6)	0.002 (5)
C15	0.038 (7)	0.035 (6)	0.062 (9)	-0.005 (5)	0.004 (6)	-0.002 (5)
C16	0.051 (8)	0.033 (6)	0.057 (9)	0.000 (5)	0.002 (6)	-0.005 (5)
C17	0.037 (7)	0.029 (6)	0.057 (8)	-0.001 (5)	0.005 (6)	-0.003 (5)
C18	0.057 (9)	0.033 (6)	0.045 (8)	0.006 (6)	-0.001 (6)	-0.008 (5)
C19	0.038 (8)	0.045 (7)	0.048 (8)	0.003 (5)	0.007 (6)	-0.001 (5)
C20	0.046 (8)	0.033 (6)	0.047 (8)	0.002 (5)	0.002 (6)	-0.002 (5)
C21	0.050 (9)	0.038 (7)	0.068 (10)	0.005 (6)	0.010 (7)	0.001 (6)
C22	0.041 (8)	0.039 (7)	0.063 (9)	0.003 (5)	0.004 (7)	0.007 (6)
C23	0.042 (8)	0.036 (7)	0.060 (9)	-0.001 (5)	0.001 (6)	-0.002 (6)
C24	0.035 (7)	0.034 (6)	0.053 (8)	0.000 (5)	0.004 (6)	0.001 (5)
C25	0.042 (8)	0.028 (6)	0.060 (9)	0.005 (5)	0.002 (6)	0.001 (5)
C26	0.035 (7)	0.027 (6)	0.064 (9)	0.003 (5)	0.003 (6)	0.000 (5)
C27	0.052 (8)	0.032 (6)	0.049 (8)	-0.005 (5)	0.008 (6)	-0.001 (5)
C28	0.047 (8)	0.037 (7)	0.059 (9)	-0.003 (5)	0.003 (7)	0.001 (5)
C29	0.058 (9)	0.039 (7)	0.070 (10)	-0.008 (6)	0.011 (7)	0.007 (6)

Geometric parameters (Å, °)

O1—C4	1.390 (16)	C15—H15	0.9800
O1—C28	1.420 (14)	C16—C17	1.519 (18)
O2—C11	1.390 (17)	C16—H16A	0.9700
O2—C29	1.432 (14)	C16—H16B	0.9700
C1—C14	1.356 (17)	C17—C26	1.393 (17)
C1—C2	1.484 (19)	C17—C18	1.407 (18)
C1—C13	1.490 (16)	C18—C19	1.371 (18)
C2—C7	1.391 (16)	C18—H18	0.9300
C2—C3	1.407 (18)	C19—C20	1.424 (17)
C3—C4	1.385 (18)	C19—H19	0.9300
C3—H3	0.9300	C20—C25	1.406 (18)
C4—C5	1.388 (16)	C20—C21	1.422 (19)
C5—C6	1.375 (19)	C21—C22	1.360 (19)
C5—H5	0.9300	C21—H21	0.9300
C6—C7	1.395 (19)	C22—C23	1.407 (19)
C6—H6	0.9300	C22—H22	0.9300
C7—C8	1.465 (19)	C23—C24	1.358 (17)
C8—C9	1.382 (16)	C23—H23	0.9300
C8—C13	1.430 (18)	C24—C25	1.427 (17)
C9—C10	1.39 (2)	C24—H24	0.9300
C9—H9	0.9300	C25—C26	1.413 (18)
C10—C11	1.375 (19)	C27—H27A	0.9600
C10—H10	0.9300	C27—H27B	0.9600
C11—C12	1.395 (17)	C27—H27C	0.9600
C12—C13	1.388 (18)	C28—H28A	0.9600
C12—H12	0.9300	C28—H28B	0.9600
C14—C26	1.474 (19)	C28—H28C	0.9600
C14—C15	1.541 (17)	C29—H29A	0.9600
C15—C27	1.524 (18)	C29—H29B	0.9600
C15—C16	1.546 (19)	C29—H29C	0.9600
C4—O1—C28	116.3 (10)	C15—C16—H16A	111.1
C11—O2—C29	117.6 (10)	C17—C16—H16B	111.1
C14—C1—C2	126.8 (11)	C15—C16—H16B	111.1
C14—C1—C13	128.4 (12)	H16A—C16—H16B	109.1
C2—C1—C13	104.7 (10)	C26—C17—C18	121.0 (11)
Continued...			

Continued...			
C7—C2—C3	120.0 (12)	C26—C17—C16	109.5 (10)
C7—C2—C1	109.9 (11)	C18—C17—C16	129.5 (11)
C3—C2—C1	130.0 (10)	C19—C18—C17	119.7 (11)
C4—C3—C2	117.8 (11)	C19—C18—H18	120.2
C4—C3—H3	121.1	C17—C18—H18	120.2
C2—C3—H3	121.1	C18—C19—C20	120.1 (12)
C3—C4—C5	122.0 (12)	C18—C19—H19	120.0
C3—C4—O1	122.6 (10)	C20—C19—H19	120.0
C5—C4—O1	115.3 (11)	C25—C20—C21	119.9 (11)
C6—C5—C4	120.2 (13)	C25—C20—C19	120.5 (11)
C6—C5—H5	119.9	C21—C20—C19	119.6 (11)
C4—C5—H5	119.9	C22—C21—C20	120.0 (13)
C5—C6—C7	118.9 (11)	C22—C21—H21	120.0
C5—C6—H6	120.5	C20—C21—H21	120.0
C7—C6—H6	120.5	C21—C22—C23	120.7 (13)
C2—C7—C6	121.1 (12)	C21—C22—H22	119.7
C2—C7—C8	108.9 (11)	C23—C22—H22	119.7
C6—C7—C8	129.9 (10)	C24—C23—C22	120.0 (12)
C9—C8—C13	119.6 (12)	C24—C23—H23	120.0
C9—C8—C7	132.6 (12)	C22—C23—H23	120.0
C13—C8—C7	107.8 (10)	C23—C24—C25	121.3 (12)
C8—C9—C10	120.3 (12)	C23—C24—H24	119.3
C8—C9—H9	119.8	C25—C24—H24	119.3
C10—C9—H9	119.8	C20—C25—C26	118.5 (11)
C11—C10—C9	119.6 (11)	C20—C25—C24	117.8 (11)
C11—C10—H10	120.2	C26—C25—C24	123.6 (12)
C9—C10—H10	120.2	C17—C26—C25	119.9 (11)
C10—C11—O2	124.7 (11)	C17—C26—C14	108.6 (10)
C10—C11—C12	122.0 (13)	C25—C26—C14	130.9 (11)
O2—C11—C12	113.3 (11)	C15—C27—H27A	109.5
C13—C12—C11	118.7 (12)	C15—C27—H27B	109.5
C13—C12—H12	120.7	H27A—C27—H27B	109.5
C11—C12—H12	120.7	C15—C27—H27C	109.5
C12—C13—C8	119.7 (10)	H27A—C27—H27C	109.5
C12—C13—C1	131.3 (11)	H27B—C27—H27C	109.5
C8—C13—C1	108.6 (11)	O1—C28—H28A	109.5
C1—C14—C26	128.7 (11)	O1—C28—H28B	109.5
Continued...			

Continued...			
C1—C14—C15	125.1 (12)	H28A—C28—H28B	109.5
C26—C14—C15	105.5 (10)	O1—C28—H28C	109.5
C27—C15—C14	114.3 (10)	H28A—C28—H28C	109.5
C27—C15—C16	110.2 (10)	H28B—C28—H28C	109.5
C14—C15—C16	100.5 (10)	O2—C29—H29A	109.5
C27—C15—H15	110.5	O2—C29—H29B	109.5
C14—C15—H15	110.5	H29A—C29—H29B	109.5
C16—C15—H15	110.5	O2—C29—H29C	109.5
C17—C16—C15	103.2 (10)	H29A—C29—H29C	109.5
C17—C16—H16A	111.1	H29B—C29—H29C	109.5
C14—C1—C2—C7	-175.1 (12)	C2—C1—C13—C8	-2.0 (13)
C13—C1—C2—C7	1.1 (13)	C2—C1—C14—C26	-167.6 (12)
C14—C1—C2—C3	8 (2)	C13—C1—C14—C26	17 (2)
C13—C1—C2—C3	-175.4 (12)	C2—C1—C14—C15	24.0 (19)
C7—C2—C3—C4	1.4 (18)	C13—C1—C14—C15	-151.3 (12)
C1—C2—C3—C4	177.6 (12)	C1—C14—C15—C27	-105.6 (14)
C2—C3—C4—C5	-2.5 (18)	C26—C14—C15—C27	83.7 (13)
C2—C3—C4—O1	-179.5 (11)	C1—C14—C15—C16	136.4 (12)
C28—O1—C4—C3	-0.5 (17)	C26—C14—C15—C16	-34.2 (12)
C28—O1—C4—C5	-177.6 (10)	C27—C15—C16—C17	-88.4 (11)
C3—C4—C5—C6	2.2 (19)	C14—C15—C16—C17	32.5 (12)
O1—C4—C5—C6	179.4 (11)	C15—C16—C17—C26	-20.7 (13)
C4—C5—C6—C7	-0.7 (19)	C15—C16—C17—C18	157.5 (12)
C3—C2—C7—C6	0.0 (18)	C26—C17—C18—C19	3.8 (18)
C1—C2—C7—C6	-177.0 (11)	C16—C17—C18—C19	-174.2 (12)
C3—C2—C7—C8	177.1 (11)	C17—C18—C19—C20	1.2 (18)
C1—C2—C7—C8	0.2 (13)	C18—C19—C20—C25	-3.0 (18)
C5—C6—C7—C2	-0.3 (19)	C18—C19—C20—C21	177.6 (11)
C5—C6—C7—C8	-176.8 (12)	C25—C20—C21—C22	3.5 (18)
C2—C7—C8—C9	177.5 (13)	C19—C20—C21—C22	-177.1 (11)
C6—C7—C8—C9	-6 (2)	C20—C21—C22—C23	1.3 (19)
C2—C7—C8—C13	-1.4 (13)	C21—C22—C23—C24	-4.6 (18)
C6—C7—C8—C13	175.4 (13)	C22—C23—C24—C25	3.1 (18)
C13—C8—C9—C10	0.3 (18)	C21—C20—C25—C26	179.1 (11)
C7—C8—C9—C10	-178.5 (13)	C19—C20—C25—C26	-0.4 (17)
C8—C9—C10—C11	2 (2)	C21—C20—C25—C24	-4.9 (17)

Continued...

Continued...

C9—C10—C11—O2	179.6 (12)	C19—C20—C25—C24	175.7 (11)
C9—C10—C11—C12	-1 (2)	C23—C24—C25—C20	1.7 (17)
C29—O2—C11—C10	-4.9 (18)	C23—C24—C25—C26	177.5 (11)
C29—O2—C11—C12	176.2 (11)	C18—C17—C26—C25	-7.2 (18)
C10—C11—C12—C13	-1.8 (19)	C16—C17—C26—C25	171.2 (11)
O2—C11—C12—C13	177.2 (11)	C18—C17—C26—C14	-179.7 (11)
C11—C12—C13—C8	4.3 (17)	C16—C17—C26—C14	-1.3 (13)
C11—C12—C13—C1	175.9 (12)	C20—C25—C26—C17	5.3 (17)
C9—C8—C13—C12	-3.6 (18)	C24—C25—C26—C17	-170.5 (11)
C7—C8—C13—C12	175.5 (11)	C20—C25—C26—C14	175.9 (11)
C9—C8—C13—C1	-177.0 (11)	C24—C25—C26—C14	0 (2)
C7—C8—C13—C1	2.1 (13)	C1—C14—C26—C17	-147.1 (12)
C14—C1—C13—C12	2 (2)	C15—C14—C26—C17	23.1 (13)
C2—C1—C13—C12	-174.3 (12)	C1—C14—C26—C25	42 (2)
C14—C1—C13—C8	174.2 (12)	C15—C14—C26—C25	-148.3 (12)

S6. Kinetics of the Thermal Helix Inversion (THI) of Motor 1 in Solution

S6.1. Kinetic Study of the Thermal Helix Inversion (THI) of 1 in Solution by ¹H-NMR

The determination of the thermodynamic parameters was done by following a reported method.^{S8} Motor 1 was dissolved in chloroform-d in an NMR tube (21 mM); the tube was then placed in an acetone/dry ice bath at a temperature of -20 °C, where it was irradiated for 10 minutes with a 370 nm 2nd generation Kessil® LED placed 6 cm away. After irradiation, the tube was placed in a second acetone/dry ice bath at -40 °C for 1 minute; then, it was placed in the 700 MHz NMR spectrometer, where it equilibrated to the spectrometer temperature for the data collection. The thermal conversions were recorded at 5 °C, 10 °C, 15 °C and 20 °C with different time intervals. The isomerization was monitored by following the doublet at $\delta = 1.4$ ppm corresponding to the rotor's methyl group (-CH₃).

Figure S5 shows the ^1H NMR of a) the stable isomer of motor **1** before irradiation, b) the appearance of the metastable isomer after irradiation for 10 minutes, and the regeneration of the stable isomer after keeping the sample in the dark for 1 h at 20 °C.

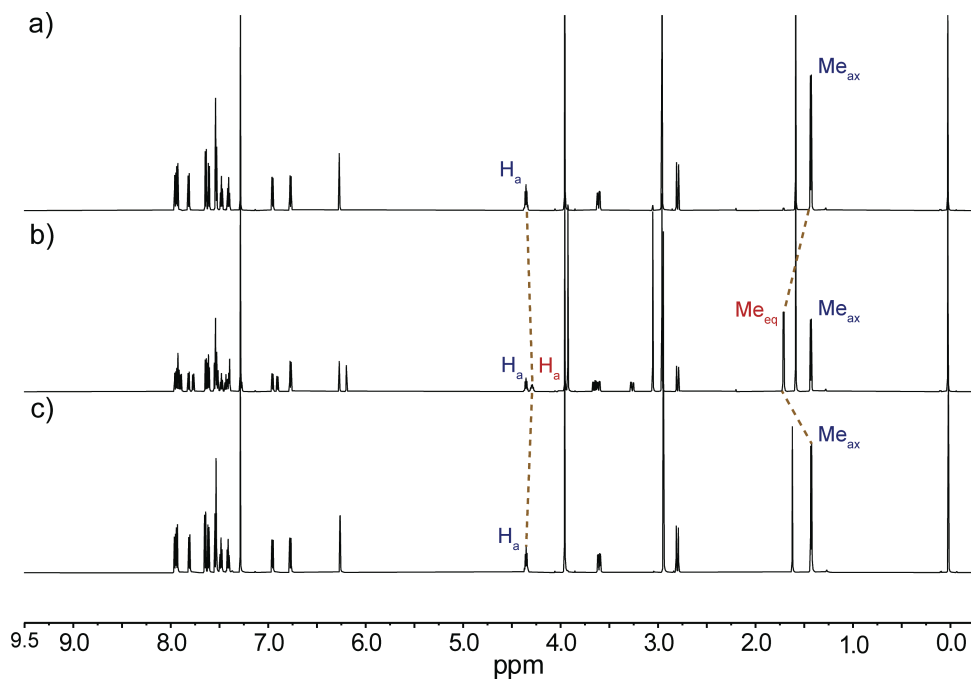


Figure S5. Full stacked ^1H NMR spectra following photoisomerization and THI of **1**. (a) before irradiation, (b) after 10 min of irradiation showing the appearance of the metastable isomer **1b**, (c) the generation of the stable isomer **1c** after keeping the sample in the dark for 1 h at 20 °C.

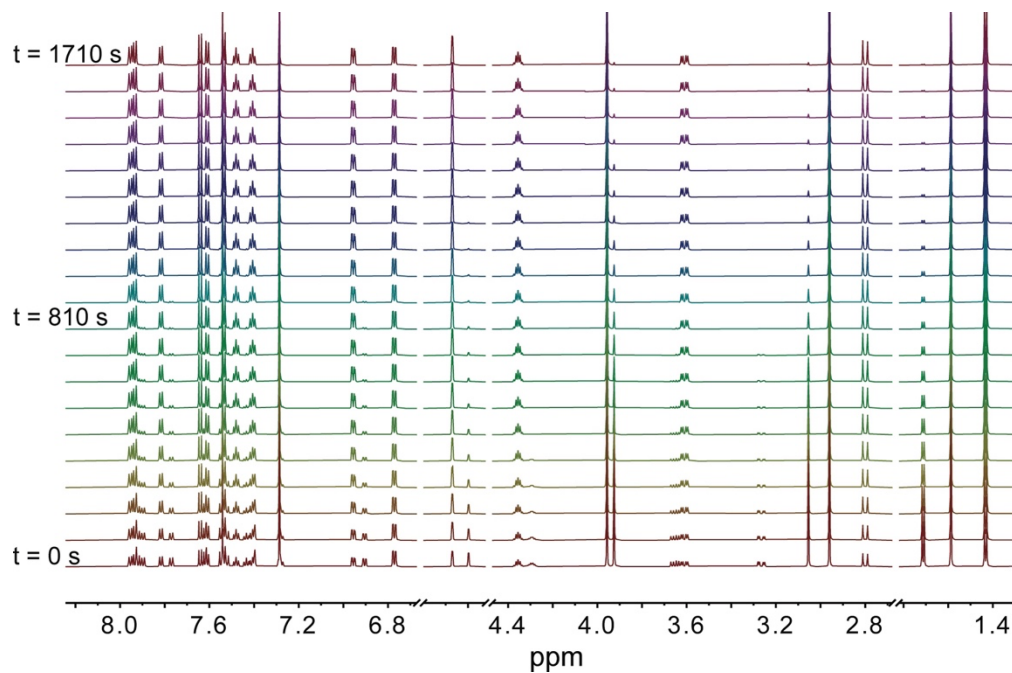


Figure S6. Example of stacked ^1H NMR spectra following THI at 20 °C in chloroform-*d*. The peak at 1.7 ppm corresponds to the methyl group in the rotor of metastable isomer **1b**. The disappearance of this peak over time indicates the generation of the stable isomer **1c** through the thermal helix inversion. Where, $t = 0$ s represents the first measurement of ^1H NMR after irradiation.

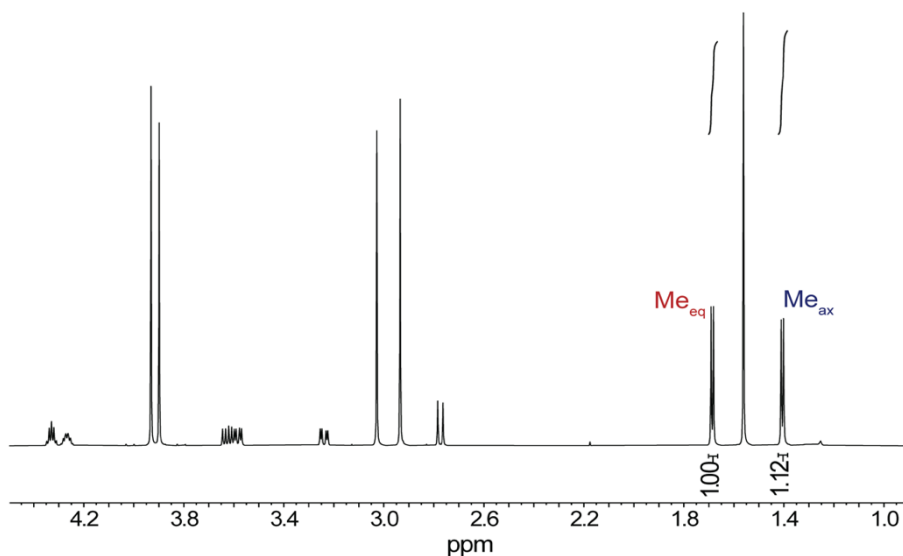


Figure S7. ^1H NMR spectrum of Motor **1** at 20 °C after irradiation with 370 nm 2nd generation kessil LED for 10 minutes at $t = 0$ s. This spectrum shows the relative integration of metastable and stable isomers' methyl peaks (Me_{ax} and Me_{eq}).

The concentration of metastable isomer [**1b**] was calculated from the integrations of the methyl peaks corresponding to metastable and stable isomers.

Metastable concentration,

$$[\mathbf{1b}]_t = \frac{x}{(x + y)} \times 21 \text{ mM at time } t \quad (\text{S2})$$

Where, x = integration of the Me_{eq} peak corresponding to the metastable isomer at a certain time and y = integration of the Me_{ax} peak corresponding to the stable isomer at a certain time. 21 mM is the total concentration motor **1**.

For example, at $t = 0$ s

$$[\mathbf{1b}]_{t=0} = \frac{1.00}{(1.00 + 1.12)} \times 21 \text{ mM}$$

$$[\mathbf{1b}]_{t=0} = 9.88 \text{ mM at } 20 \text{ }^\circ\text{C}$$

Similarly, metastable concentrations were calculated for each 90 s intervals at 20 °C up to 20 experiments. The metastable concentrations [**1b**] were plotted against time (s) and a first-order exponential decay curve was observed (**Figure 3a**), which indicates the conversion of the metastable isomer (**1b**) to the stable isomer (**1c**). The plot of the natural logarithm of [**1b**] vs time (s) gave a linear decay (**Figure 3b**). The slope of the linear fit corresponds to the rate constant (k). The half-life ($t_{1/2}$) was calculated by following first-order kinetics.

$$\begin{aligned}t_{1/2} &= \frac{0.693}{k} \text{ s} && \text{(S3)} \\ &= \frac{0.693}{0.00205} \text{ s} \\ &= 338 \text{ s}\end{aligned}$$

Similarly, the rate constant and the half-life were calculated at 5 °C, 10 °C and 15 °C (**Figure S8**).

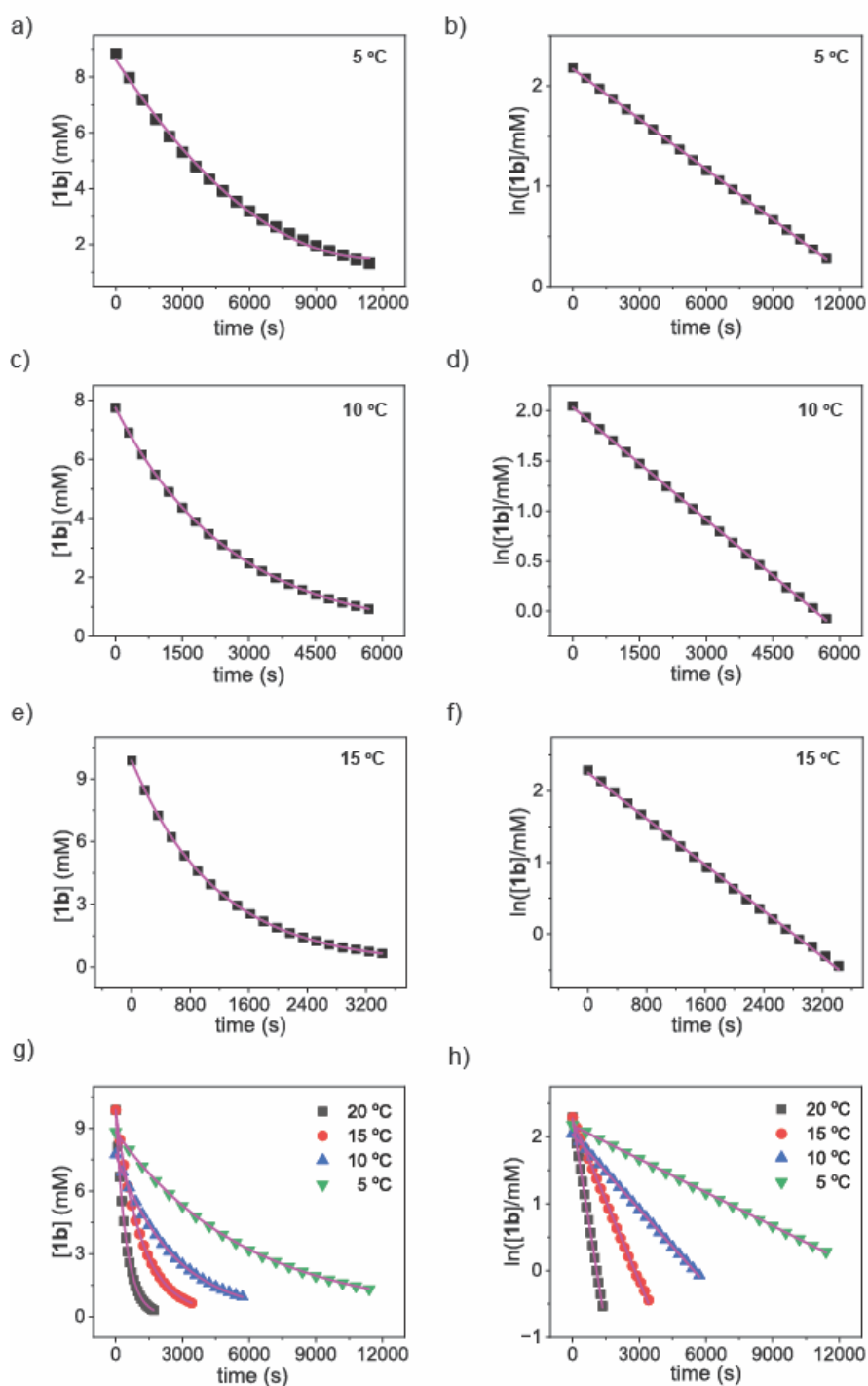


Figure S8. Thermal isomerization of **1** at different temperatures in chloroform-d. The metastable concentration was determined by integrating of the metastable and stable isomers peaks. Exponential decay was observed by plotting **[1b]** vs time (s) (a, c, e, g) and linear decay was observed by plotting the natural logarithm of **[1b]** vs time (s) (b, d, f, h), where (a) and (b) represent 5 °C, (c) and (d) represent 10 °C, (e) and (f) represent 15 °C (i) Comparison of **[1b]** vs time (s) at 20, 15, 10 and 5 °C. (j) Comparison of $\ln[1b]$ vs time (s) at 20, 15, 10 and 5 °C.

The standard values of the thermodynamic parameters such as enthalpy, entropy, and Gibb's free energy of the THI of motor **1** were determined by the Eyring analysis. The natural logarithm of the ratio of rate constant and temperature ($\ln \frac{k}{T}$) was plotted vs the reciprocal of temperature ($1/T$) resulting in a linear decay. By treating the Eyring equation (**Equation S4**) as a linear equation, $y = mx + c$, the enthalpy can be extracted from the slope (m) (**Equation S5**) and the entropy from the intercept (c) (**Equation S6**).

$$\text{Eyring equation, } \ln \frac{k}{T} = -\frac{\Delta^\ddagger H^\circ}{R} \cdot \frac{1}{T} + \ln \frac{k_B}{h} + \frac{\Delta^\ddagger S^\circ}{R} \quad (\text{S4})$$

Here, k is the rate constant, T is the temperature in Kelvin, $\Delta^\ddagger H^\circ$ is the enthalpy of activation, $\Delta^\ddagger S^\circ$ is entropy, R is the gas constant, k_B is the Boltzmann constant, h is the Planck's constant.

$$R = 1.987 \text{ cal/mol.K}$$

$$k_B = 1.38065 \times 10^{-23} \text{ m}^2.\text{kg/s}$$

$$h = 6.626 \times 10^{-34} \text{ m}^2.\text{kg/s}$$

$$\text{slope, } m = -\frac{\Delta^\ddagger H^\circ}{R} = -13234.63 \quad (\text{S5})$$

$$\Delta^\ddagger H^\circ = 26.29 \text{ kcal/mol at } 293 \text{ K}$$

$$\text{intercept, } c = \ln \frac{k_B}{h} + \frac{\Delta^\ddagger S^\circ}{R} = 33.24 \quad (\text{S6})$$

$$\Delta^\ddagger S^\circ = 18.84 \frac{\text{cal}}{\text{mol} \cdot \text{K}}$$

Furthermore, the Gibb's free energy ($\Delta^\ddagger G^\circ$) of activation was calculated from the thermodynamic equation of the free energy (**Equation S7**).

$$\Delta^\ddagger G^\circ = \Delta^\ddagger H^\circ - T\Delta^\ddagger S^\circ \quad (\text{S7})$$

$$\Delta^\ddagger G^\circ = 20.72 \text{ kcal/mol at 293 K}$$

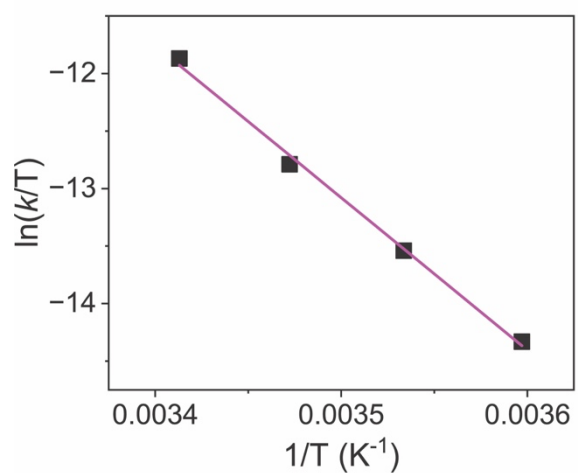


Figure S9. Eyring plot for the data collected by NMR in chloroform-*d*.

Table S2. Thermodynamic parameters calculated using the Eyring Plot.

$\Delta^\ddagger G^\circ$ (kcal/mol)	$\Delta^\ddagger H^\circ$ (kcal/mol)	$\Delta^\ddagger S^\circ$ (cal/mol·K)	Solvent	Method
20.72	26.29	18.84	chloroform- <i>d</i>	NMR

Table S3. Kinetic parameters of the THI in solution determined by NMR in chloroform-d at different temperatures.

T	k ($s^{-1} \times 10^{-5}$)	$t_{1/2}$ (s)	ω (mHz)
20 °C	205 ± 1.0	338 ± 1.0	1.0
15 °C	80 ± 3.0	863 ± 0.2	0.4
10 °C	37 ± 1.0	1858 ± 1.0	0.2
5 °C	17 ± 2.0	4157 ± 0.4	0.1

Furthermore, we also determined the kinetic parameters of the THI in acetone- d_6 at 20 °C using the same procedure as in chloroform-d (**Figure S10**). The rate constant and half-life of the thermal helix inversion step were determined to be 0.00265 s^{-1} and 261 s, respectively.

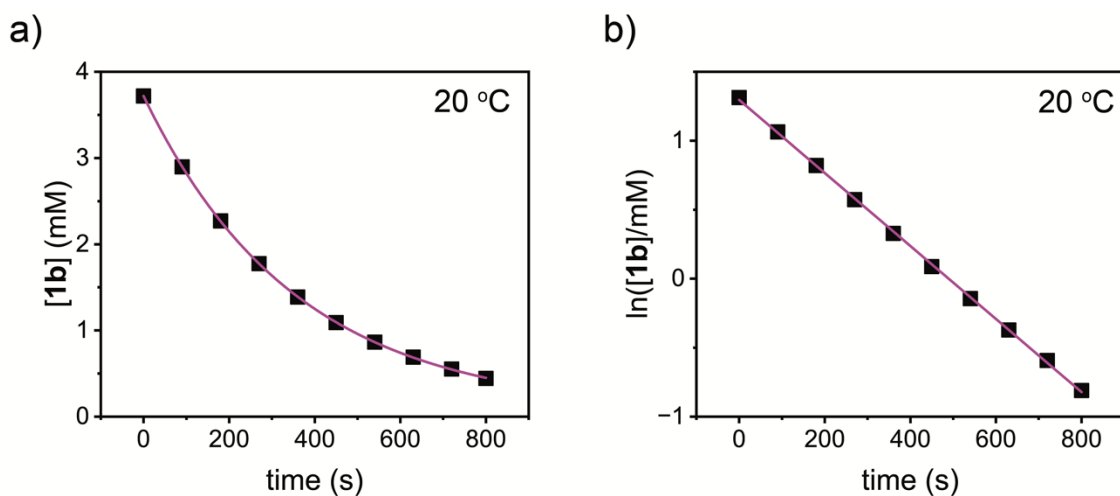


Figure S10. Thermal isomerization of **1** at 20 °C in acetone- d_6 . The metastable concentration was determined by integrating the metastable and stable isomer peaks. Exponential decay was observed by plotting [1b] vs time (s) and linear decay was observed by plotting the natural logarithm of [1b] vs time (s).

S6.2. Kinetic Study of the Thermal Helix Inversion (THI) of **1** in Solution by UV-Vis Spectroscopy

UV-Vis experiments were performed using an Agilent 8453 Diode array UV-Vis

spectrophotometer. Motor **1** was dissolved in the chosen solvent (acetone or chloroform,) at a concentration of $1 \times 10^{-4} \text{ mol L}^{-1}$ and irradiated for 5 min using a 370 nm 1st generation Kessil[®] LED placed at a distance of 10 cm from the middle of a 70 μL Brand[®] UV-cuvette with the long axis of the sample cuvette perpendicular to the irradiation beam. Once irradiated for 5 min, the cuvette was then transferred to the UV-Vis spectrometer, and the first spectrum was recorded within 10 s from the stop of irradiation. The spectrum was recorded against the appropriate solvent baseline for studies of **1** in solution. Spectra were recorded from 300 to 750 nm with an integration time of 1 s and a resolution of 1 nm. Spectra were recorded at intervals of 0.5 min until $t = 5$ min and then at intervals of 1 min. Each spectrum was then cut at 350 nm and fitted using two Gaussian functions which resolved into a stable state around 387 nm and a peak for the metastable state around 413 nm. The area of the peaks was then used to determine k via first order kinetics treatment. Three independently prepared samples were averaged to obtain the final values. A detailed procedure used to fit the absorbance peaks is given in the next section. Once adjusted for irradiation during measurement of the spectrum (**Section S7.1**), the natural log of the metastable state concentration allowed determination of the Thermal Helix Inversion (THI) rate, half-life, and rotation frequency of Motor **1** in each solvent.

S7. Kinetic Study of the Thermal Helix Inversion (THI) of Motor 1 in Polymersomes

UV-Vis experiments were performed using an Agilent 8453 Diode array UV-Vis spectrophotometer. Polymersomes prepared at a diblock copolymer concentration of $5 \times 10^{-3} \text{ mol L}^{-1}$ and a concentration of **1** of $1.0 \times 10^{-4} \text{ mol L}^{-1}$ was used for the kinetic study of the Thermal Helix Inversion (THI) of motor **1** within polymersomes. The spectra were recorded against a pure PDMS₁₃-*b*-PEG₁₃ polymersome baseline (Sample 100:0). Unless otherwise stated,

irradiation and spectroscopy took place at ambient temperature (21 °C). During irradiation, the sample cuvette was placed in a small cylindrical cuvette within a water bath for temperature control during irradiation. After irradiation for 5 min, the sample was transferred to the spectrophotometer. The amount of motor in the metastable state was calculated by comparing the areas of the fit functions for the stable and metastable states at a given time. The proportion of the metastable state was calculated according to:

$$\text{proportion of } 1b = \frac{\text{Area Gauss}_{1b}}{\text{Area Gauss}_{1c} + \text{Area Gauss}_{1b}} \quad (\text{S8})$$

The results of three independently prepared samples were averaged to obtain the final values.

S7.1. Procedure for Fitting Absorbance Peaks

The stable isomer of this Feringa-type motor shows a maximum absorption at about 387 nm, while the metastable isomer has a maximum absorption at about 413 nm. As recording a spectrum with a 100 % metastable state was not possible at ambient temperatures given the time necessary to transfer the sample from the irradiation station to the spectrophotometer. A spectrum of each sample recorded before irradiation was fitted to find the peak maximum wavelength and full width at half maximum (FWHM) of the peak for the stable state. These parameters were kept fixed for all further fits of a given sample. The first spectrum recorded during each experiment was then fitted to find the shape parameters of the Gaussian distribution representing the peak for the metastable state. The peak maximum and full width at half maximum (FWHM) of the peak for the metastable state were then kept constant for the remaining fits of a given sample.

Figure S11 shows the absorbance vs wavelength for motor **1** in the polymersome, recorded as soon as the sample was placed in the spectrophotometer following irradiation. The sample

contains a diblock copolymer concentration of $5 \times 10^{-3} \text{ mol L}^{-1}$ and a motor **1** concentration of $1.0 \times 10^{-4} \text{ mol L}^{-1}$. The markings on the spectrum represents an example of the fitting procedure. The thick grey line shows the original experimental data, after subtracting the instrumental baseline that varies slightly with each measurement. As all spectra have been recorded against the appropriate solvent of the diblock copolymer baseline, this step does not consider changes in the spectrum from scattering off larger particles. The red (short dashes) and blue (dotted) lines, represent the individual Gaussian distributions, and the black (long dashes) line the sum of both peaks. The blue (dotted) and red (short dashes) lines represent the stable and metastable states, respectively. In this example, most of **1** (77 %) is in a metastable state. 23 % is in the stable state. Correlation coefficients remained at a high 0.997 or higher for all fits.

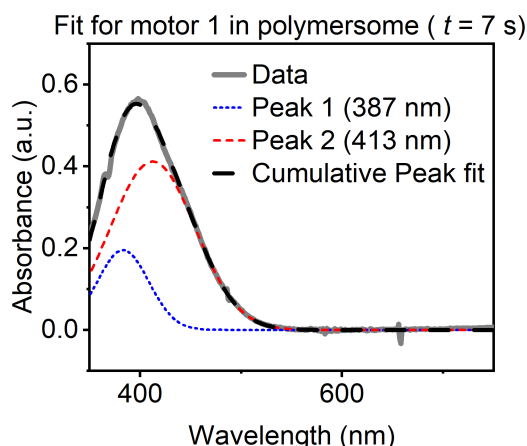


Figure S11. Example of a fit for motor **1** in the polymersome. The spectrum was recorded at $t = 7 \text{ s}$ after irradiation. The recorded spectrum with subtracted baseline (grey), the stable state peak at 387 nm (blue, dotted), the metastable state peak at 413 nm (red, short dashes), and the cumulative fit (black, long dashes) are shown. The shown sample contains 77 % metastable state and 23 % stable state.

S8. Effect of temperature fluctuations during DLS measurements

During irradiation with light, we observed the sample temperature increased from $22 \text{ }^\circ\text{C}$ to $24 \text{ }^\circ\text{C}$ and remained constant over time (**Figure S12a**). Therefore, we separately studied the effect of temperature on the D_H . We observed a slight decrease in the diameter when heating the samples

(Figure S12b). Therefore, if the DLS data is collected at 22 °C, but the sample is at 24 °C due to the light irradiation, we would falsely observe an increase in D_H over time the sample is measured (Figure S13a). So, immediately after irradiation, the diameter is smaller, but it increases as the sample cools down and reaches the same temperature of the instrument (22 °C). Upon equilibration, the diameter remains constant at 22 °C.

Such behavior is attributed to the changes in viscosity with temperature, which the software does not adjust when determining D_H (equation S1). However, if we compare the values where D_H is constant (upon equilibration at 22 °C), and the values before light irradiation, we can observe there is no change in size before and after irradiation (Table S4). Likewise, the PDI remains constant.

Thus, to avoid this phenomenon and simplify our analysis, we set up the DLS instrument at 24°C when measuring the samples irradiated with light (data presented in main text Figure 7a and Table 3).

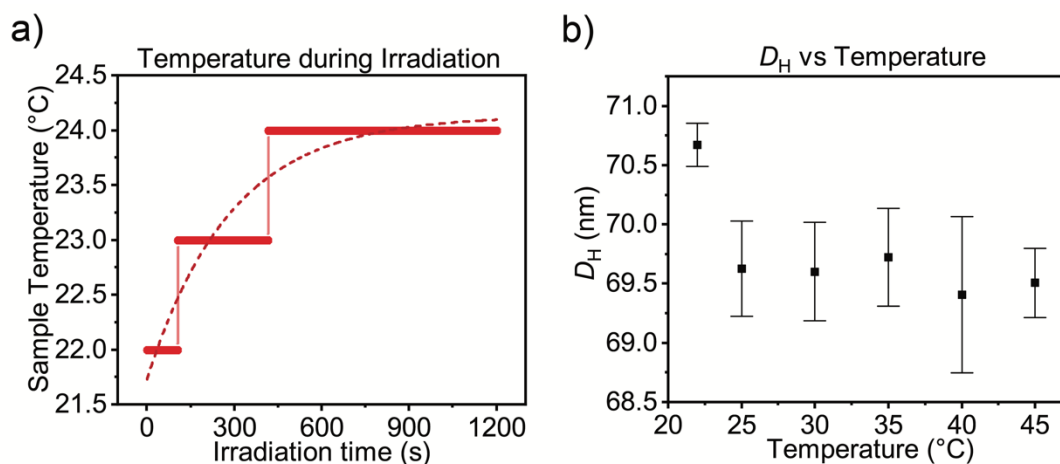


Figure S12. a) Increase in temperature of the polymersome sample during irradiation. b) A decrease in diameter is observed when heating the polymersome sample from 22 °C to higher temperatures.

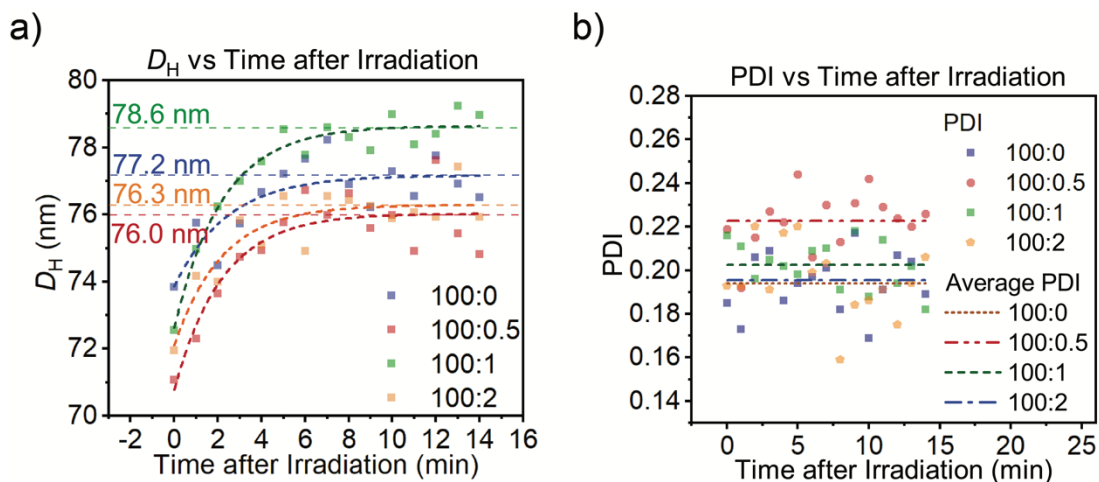


Figure S13. a) Hydrodynamic Diameter (D_H) and b) polydispersity index (PDI) of the polymersomes with different amounts of motors after 5 min of light irradiation measured at 22 °C. Cumulant fit error bars are smaller than the symbol size and were omitted for clarity.

Table S4. Hydrodynamic Diameter (D_H) and polydispersity index (PDI) of polymersomes incorporated with different concentrations of motor **1** after 5 min of light irradiation measured at 22 °C.

Diblock copolymer:motor molar ratio	D_H before irradiation (nm)	Final D_H after irradiation (nm)	PDI
100:0	77.5 ± 0.4	77.2 ± 0.3	0.19 ± 0.01
100:0.5	76.4 ± 1.2	76.3 ± 0.3	0.22 ± 0.01
100:1	78.5 ± 0.5	78.6 ± 0.2	0.20 ± 0.01
100:2	77.1 ± 0.2	76.3 ± 0.3	0.19 ± 0.02

S9. NMR Spectra

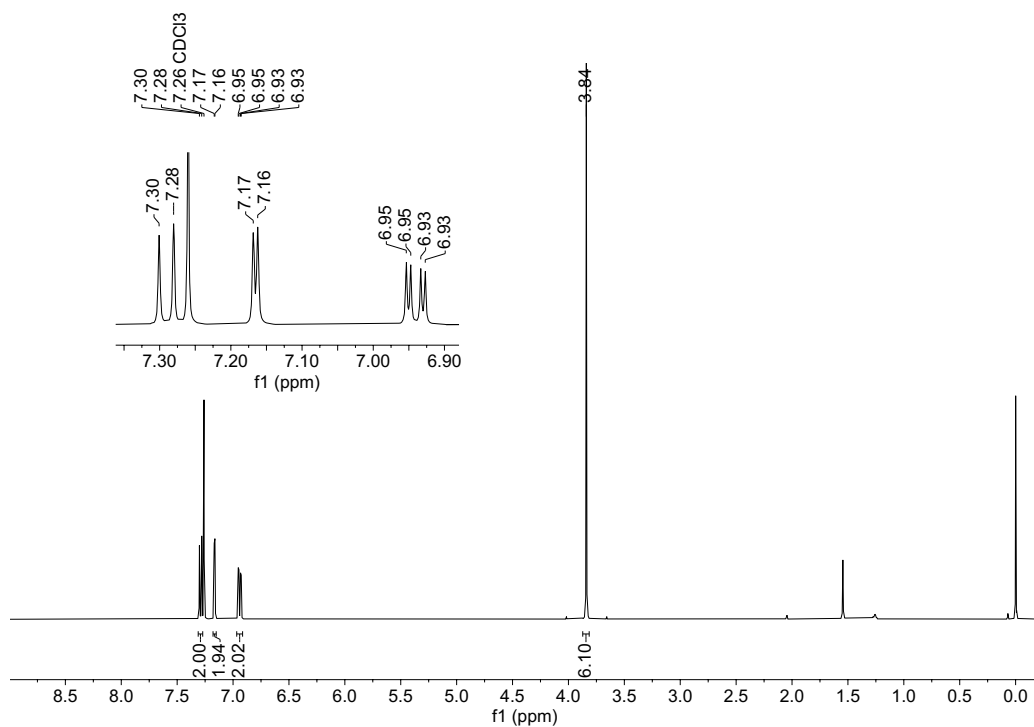


Figure S14. ¹H NMR spectrum (400 MHz, $T = 297$ K) of **4** in chloroform-d.

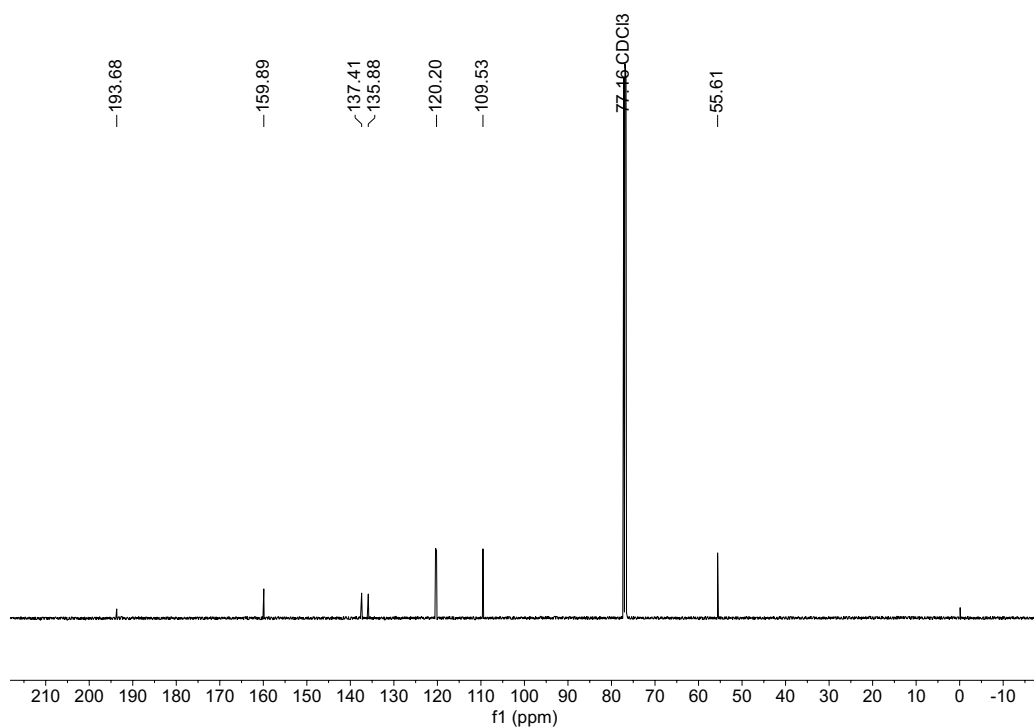


Figure S15. ¹³C NMR spectrum (500 MHz, $T = 297$ K) of **4** in chloroform-d.

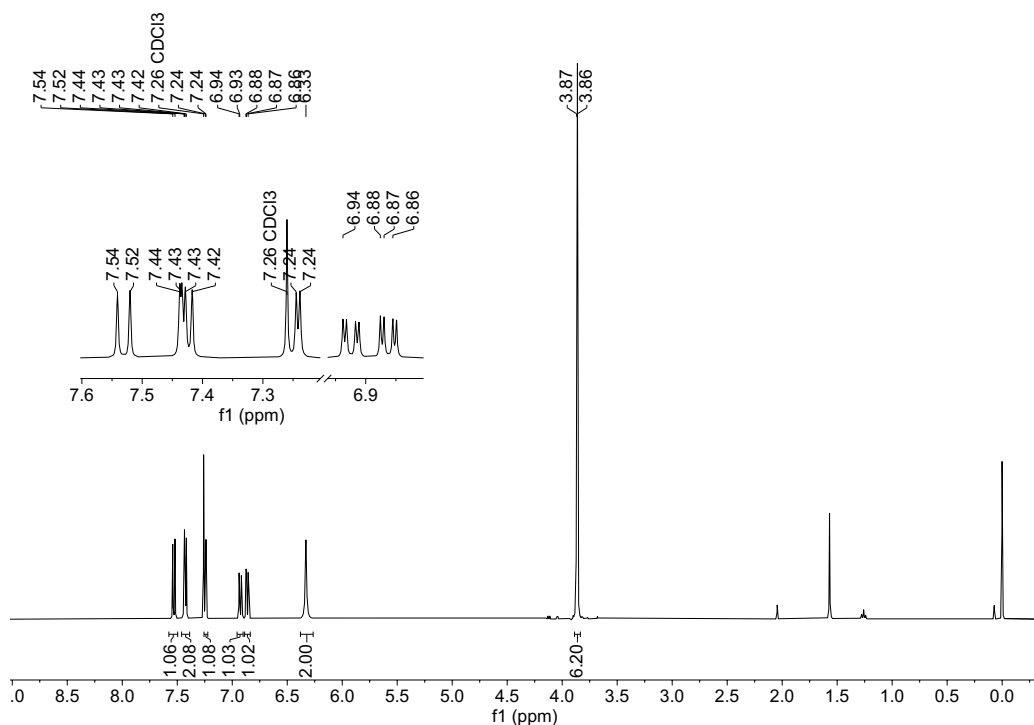


Figure S16. ^1H NMR spectrum (400 MHz, $T = 297$ K) of **6** in chloroform-d.

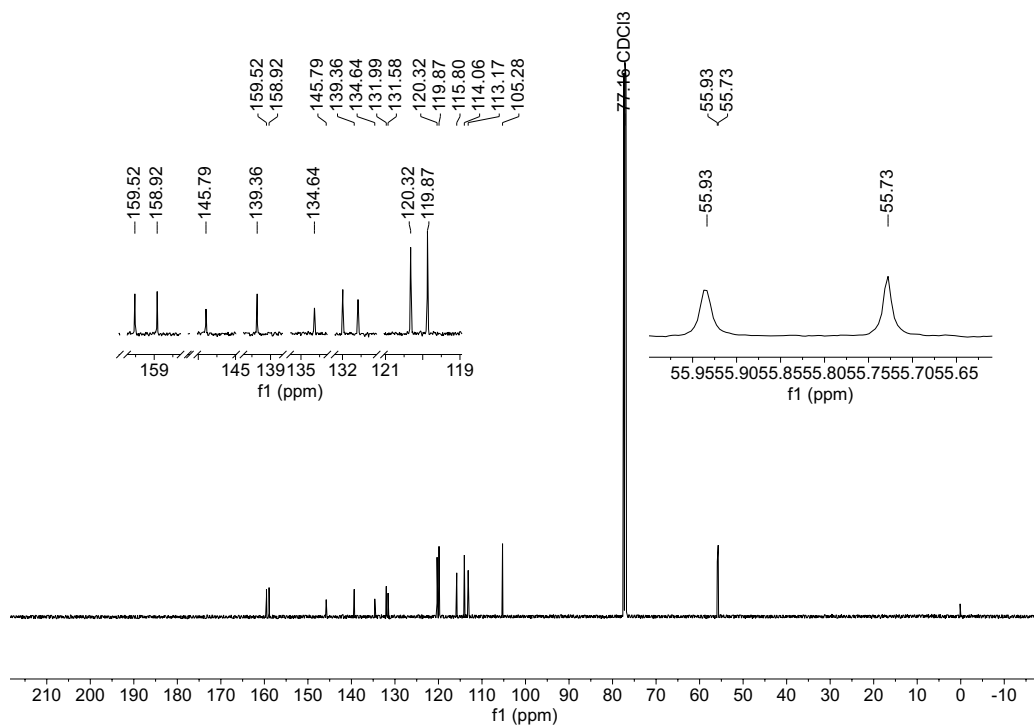


Figure S17. ^{13}C NMR spectrum (500 MHz, $T = 297$ K) of **6** in chloroform-d.

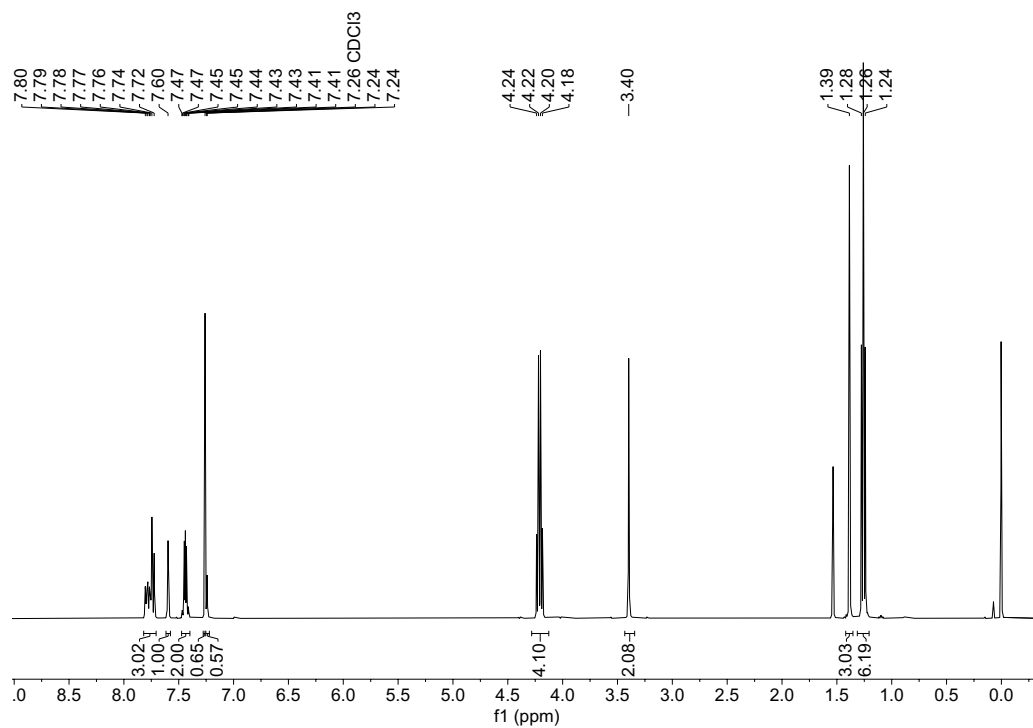


Figure S18. ^1H NMR spectrum (400 MHz, $T = 297$ K) of **12** in chloroform-d.

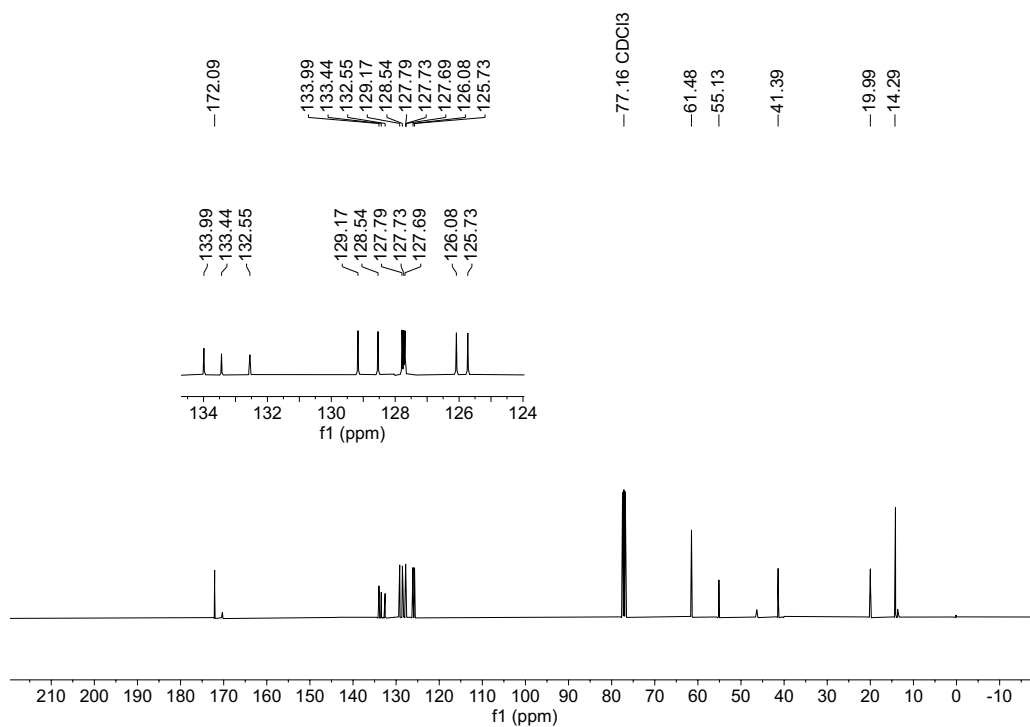


Figure S19. ^{13}C NMR spectrum (500 MHz, $T = 297$ K) of **12** in chloroform-d.

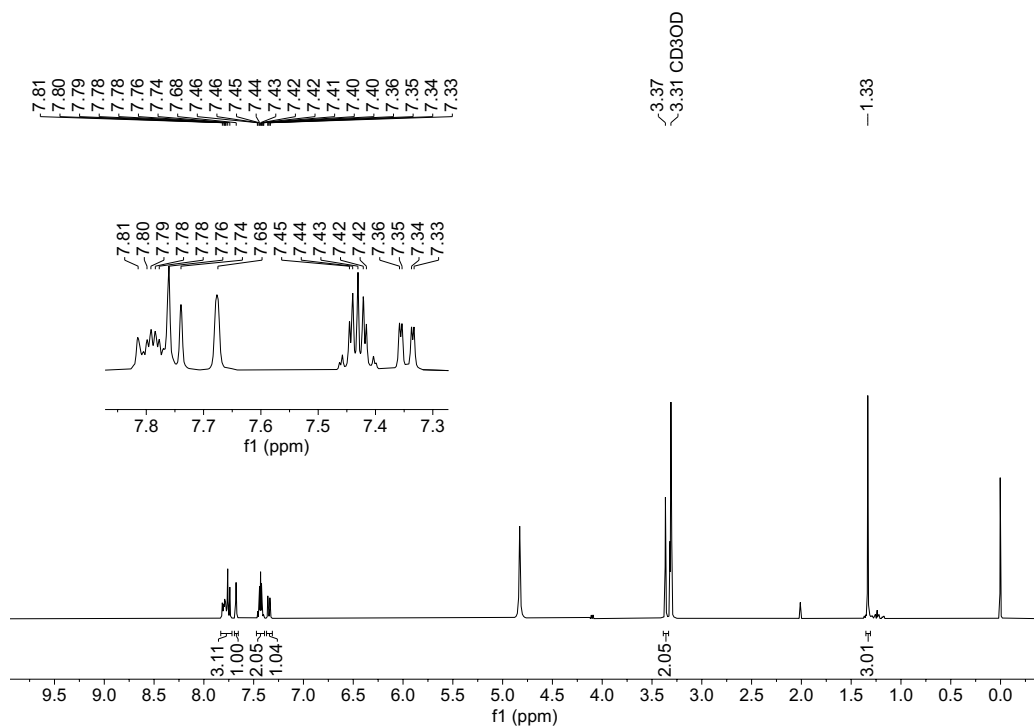


Figure S20. ^1H NMR spectrum (400 MHz, $T = 297$ K) of **13** in methanol-d.

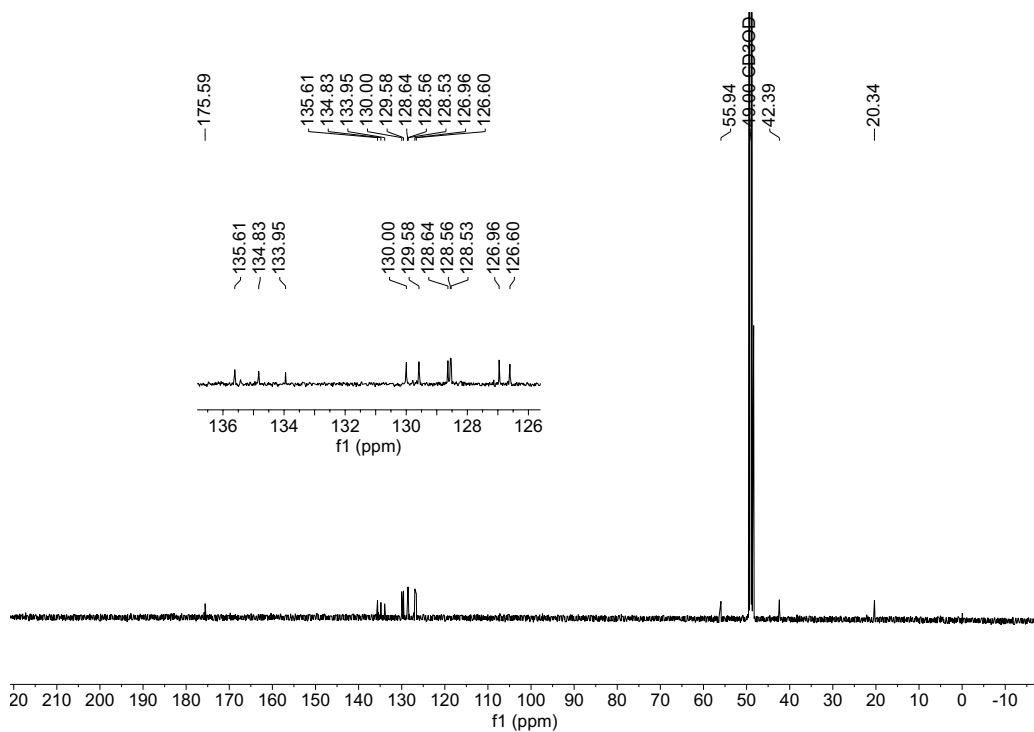


Figure S21. ^{13}C NMR spectrum (500 MHz, $T = 297$ K) of **13** in methanol-d.

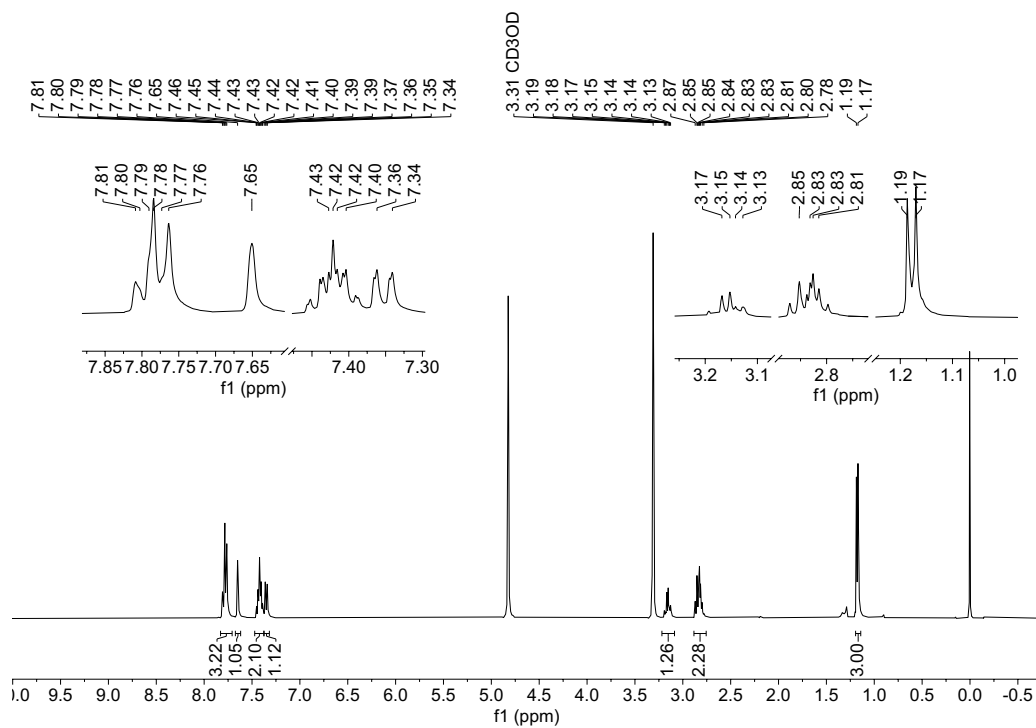


Figure S22. ¹H NMR spectrum (400 MHz, *T* = 297 K) of **14** in methanol-d.

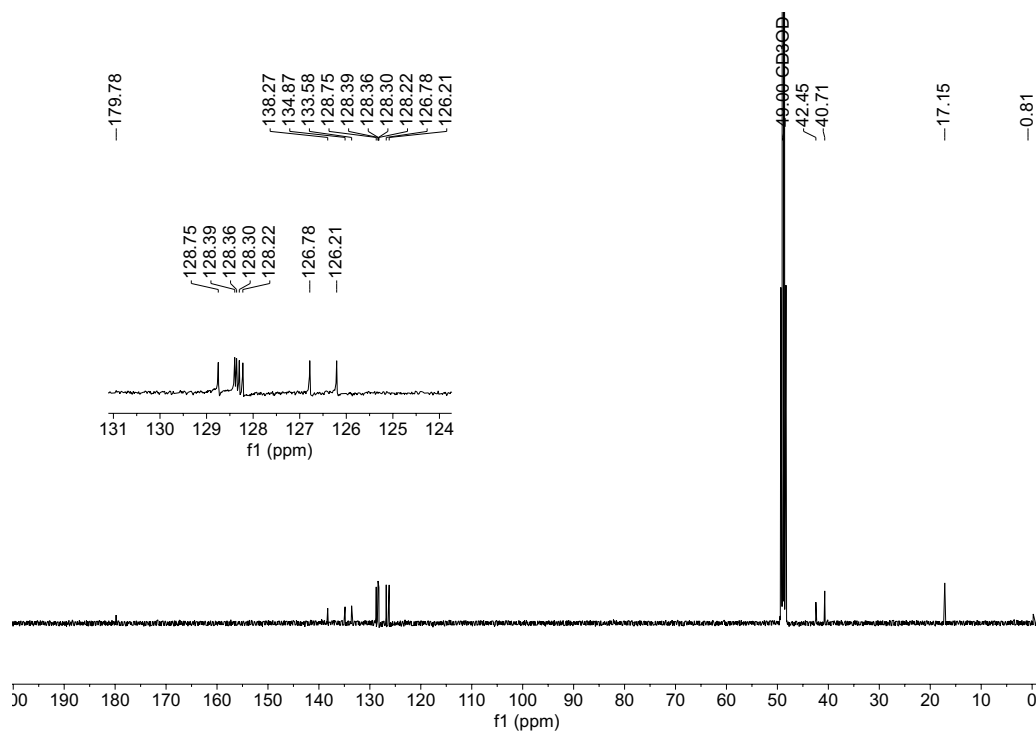


Figure S23. ¹³C NMR spectrum (400 MHz, *T* = 297 K) of **14** in methanol-d.

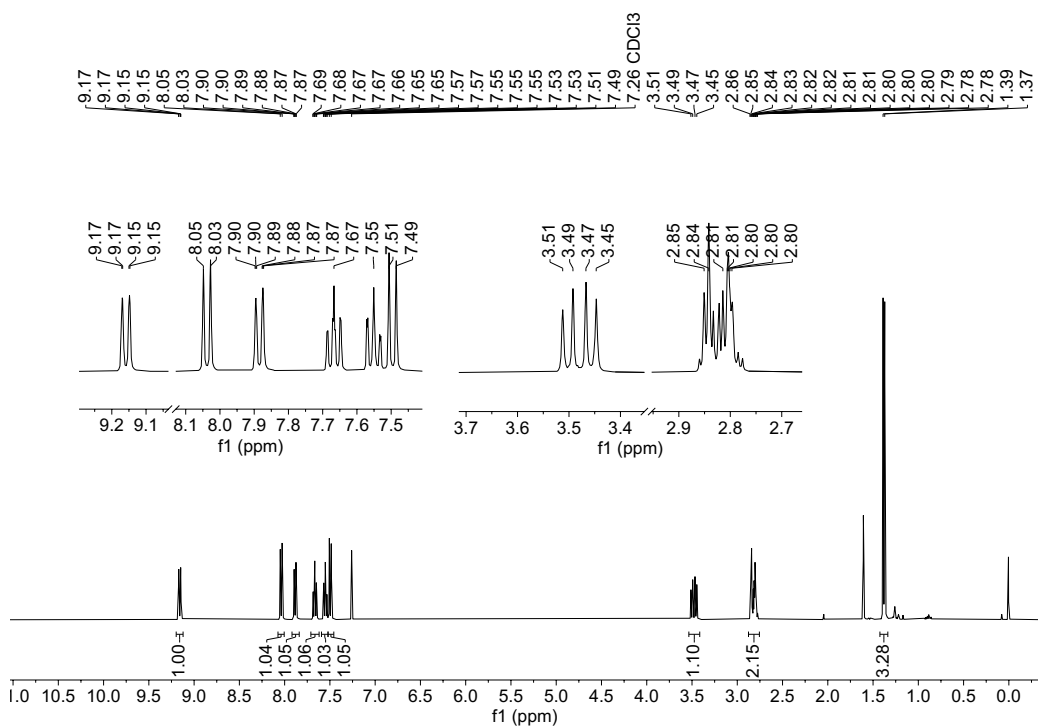


Figure S24. ^1H NMR spectrum (400 MHz, $T = 297$ K) of **15** in chloroform- d .

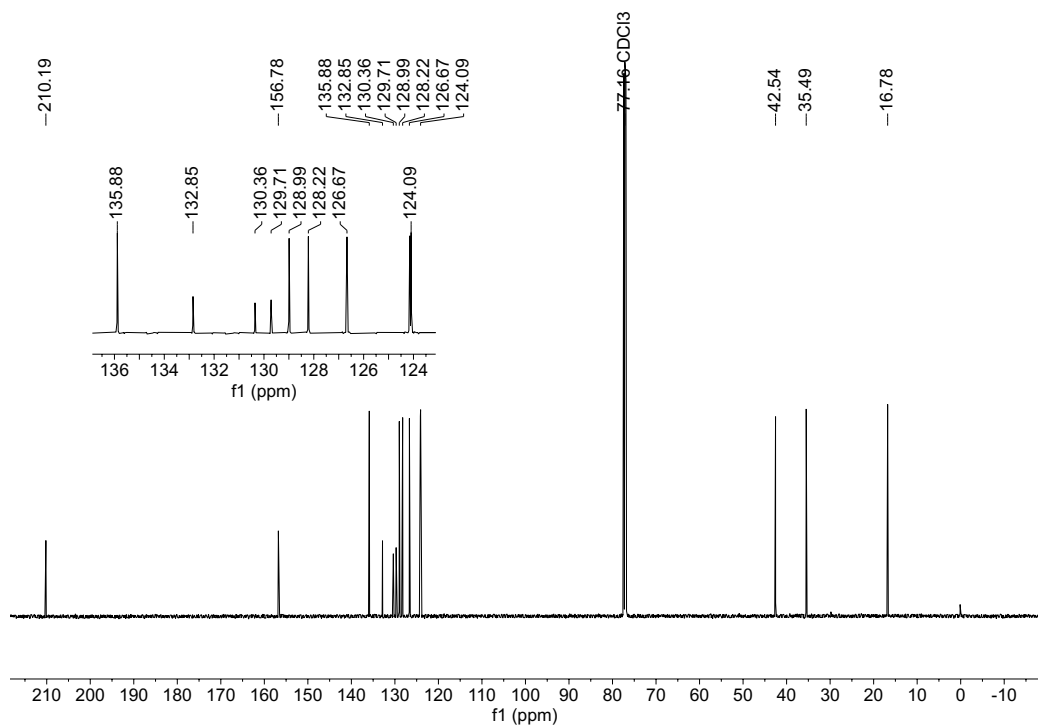


Figure S25. ^{13}C NMR spectrum (500 MHz, $T = 297$ K) of **15** in chloroform- d .

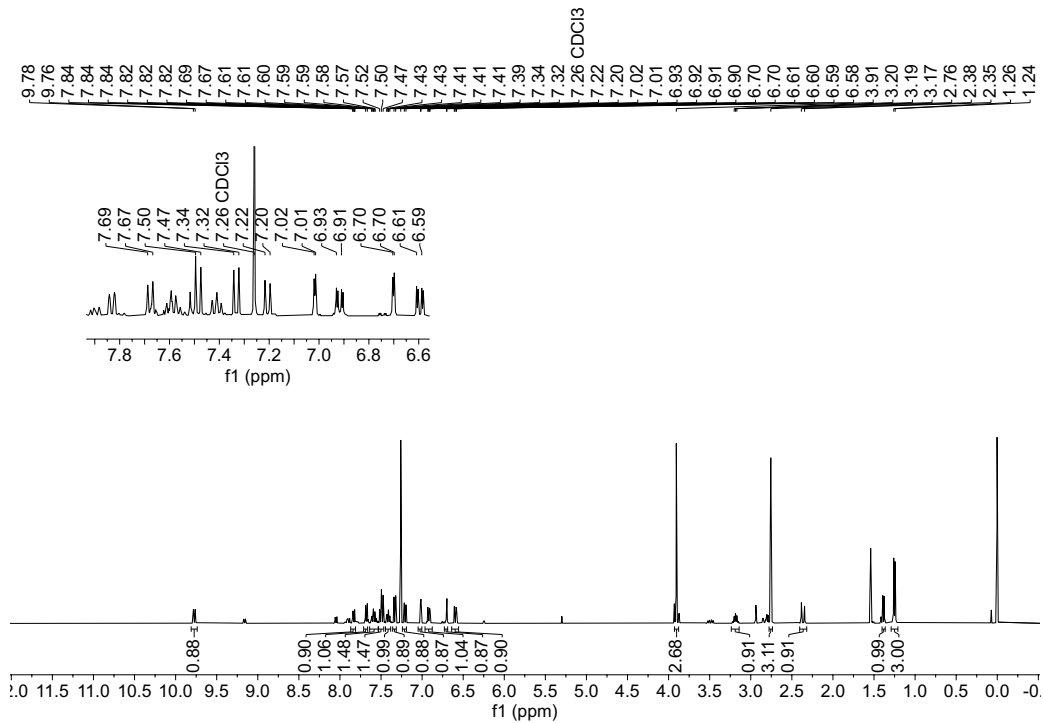


Figure S26. ¹H NMR spectrum (400 MHz, *T* = 297 K) of **8** in chloroform-d.

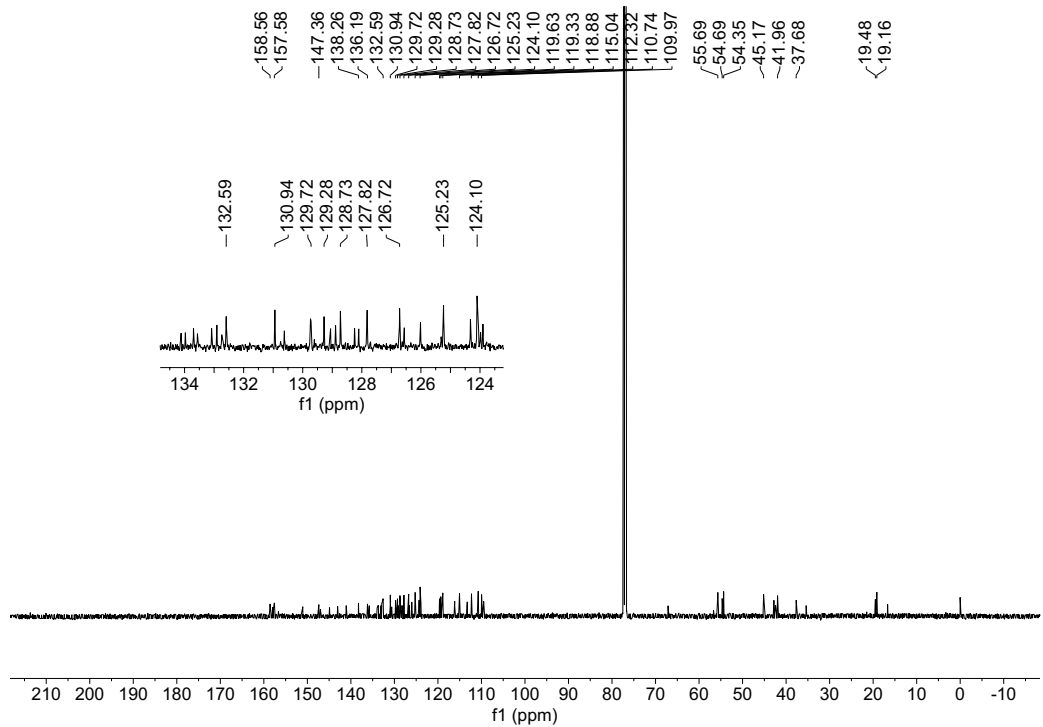


Figure S27. ¹³C NMR spectrum (500 MHz, *T* = 297 K) of **8** in chloroform-d.

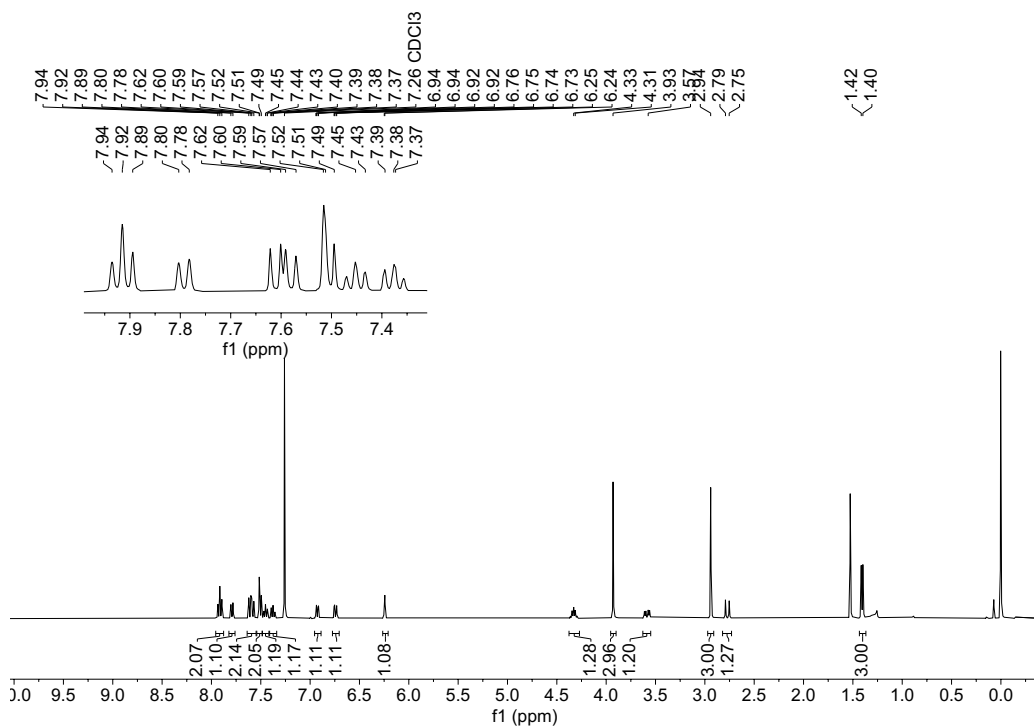


Figure S28. ^1H NMR spectrum (400 MHz, $T = 297$ K) of **1** in chloroform-d.

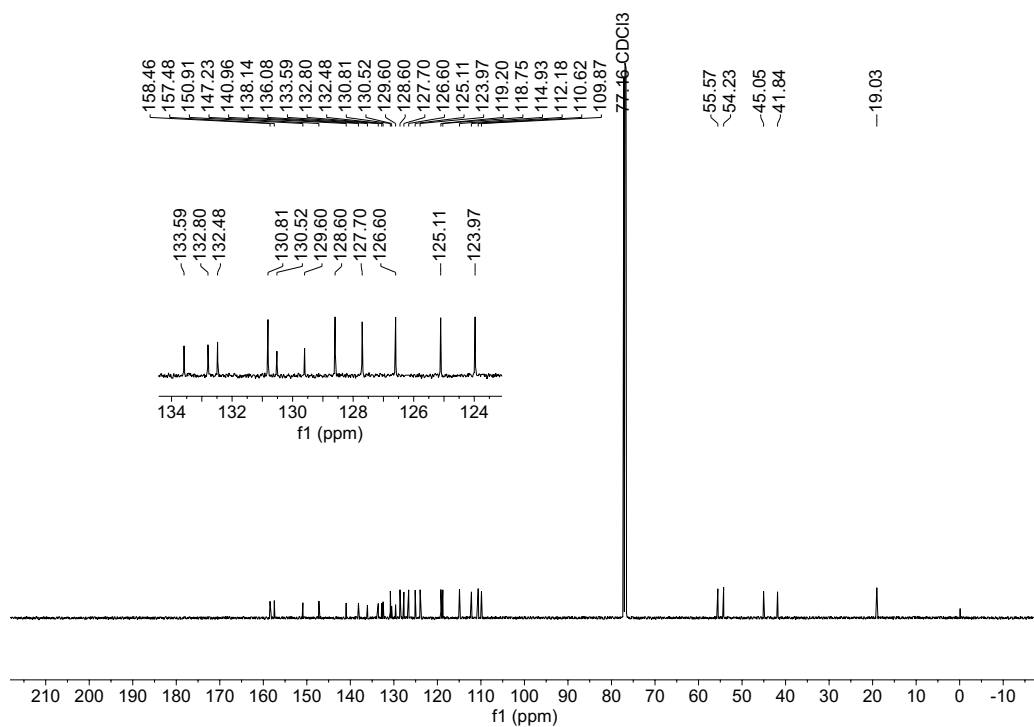


Figure S29. ^{13}C NMR spectrum (500 MHz, $T = 297$ K) of **1** in chloroform-d.

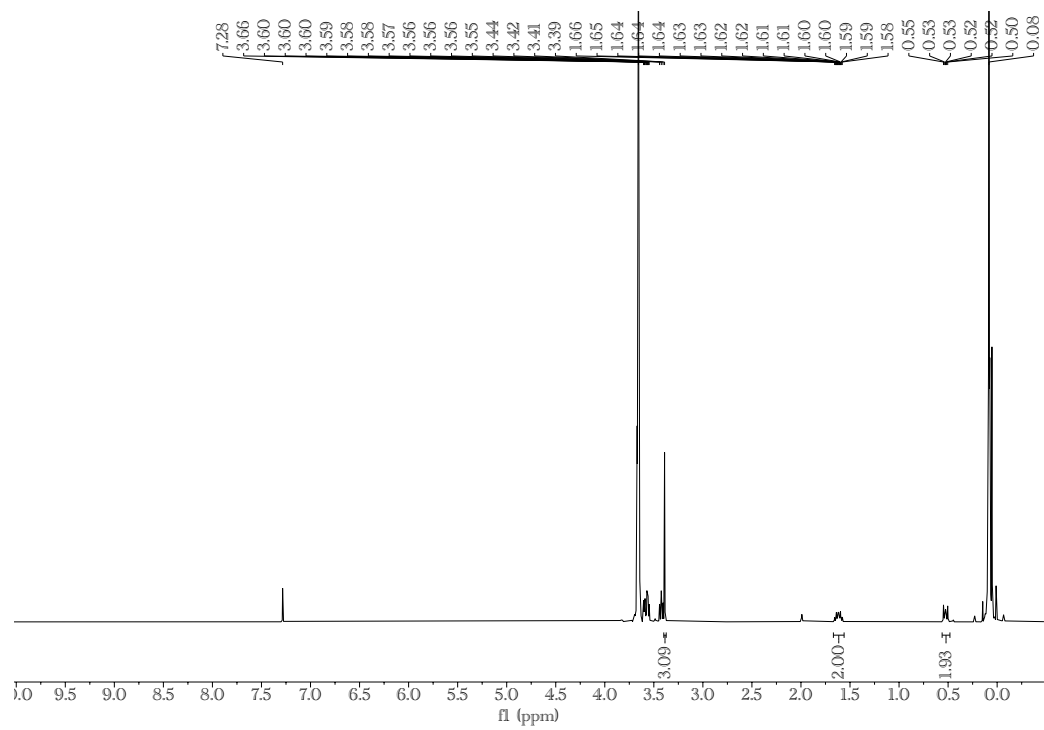


Figure S30. Full spectrum of copolymer **2**.

Supplemental References

- S1 T. Ozturk, E. Ertas and O. Mert, *Chem. Rev.*, 2007, **107**, 5210-5278.
- S2 Q. Li, J. T. Foy, J. R. Colard-Itté, A. Goujon, D. Dattler, G. Fuks, E. Moulin and N. Giuseppone, *Tetrahedron*, 2017, **73**, 4874-4882.
- S3 H. Tsuji, K. Hashimoto and M. Kawatsura, *Org. Lett.*, 2019, **21**, 8837-8841.
- S4 P. H. Gore, *Chem. Rev.*, 1955, **55**, 229-281.
- S5 R. M. Perera, S. Gupta, T. Li, M. Bleuel, K. Hong and G.J. Schneider, *Soft Matter*, 2021, **17**, 4452-4463.
- S6 J. U. De Mel, S. Gupta, R. M. Perera, L. Ngo, P. Zolnierczuk, M. Bleuel, S. V. Pingali and G. J. Schneider, *Langmuir*, 2020, **36**, 9356-9367.
- S7 L. Krause, R. Herbst-Irmer, G. M. Sheldrick and D. Stalke, *J. Appl. Cryst.*, 2015, **48**, 3-10.
- S8 A. van Venrooy, A. M. Wyderka, V. García-López, L. B. Alemany, L. A. A. Marti and J. M. Tour, *J. Org. Chem.*, 2023, **88**, 762-770.